# PRESSURE AND STRESS DISTRIBUTION ANALYSIS OF CENTRIFUGAL PUMP

Thesis submitted in partial fulfilment of the requirements for the award of degree of

**Master of Engineering**

in

**CAD/CAM & ROBOTICS**

**Thapar University, Patiala**


By:

**Karan Rajdev**

**Roll No. 80681011**

Under the supervision of:

**Mr. Satish Kumar**

Lecturer, MED

**Mr.Kishore Khanna**

MED


**JUNE 2008**


MECHANICAL ENGINEERING DEPARTMENT

THAPAR UNIVERSITY

PATIALA – 147004

# CERTIFICATE

I hereby certify that the work which is being presented in the thesis entitled, "**PRESSURE AND STRESS DISTRIBUTION ANALYSIS OF CENTRIFUGAL PUMP** ", in partial fulfilment of the requirements for the award of degree of Master of Engineering in Mechanical Engineering with specialization in **CAD/CAM & ROBOTICS** submitted in **Mechanical Engineering Department** of Thapar University, Patiala, is an authentic record of my own work carried out under the supervision of Mr. **Satish Kumar** and refers other researcher's works which are duly listed in the reference section.

The matter presented in this thesis has not been submitted for the award of any other degree of this or any other university.

**Karan Rajdev**

This is to certify that the above statement made by the candidate is correct and true to the best of my knowledge.


**Satish Kumar**
Lecturer, MED
Thapar University
Patiala

**Kishore Khanna**
MED
Thapar University
Patiala

**Dr .S.K MOHAPATRA**
Professor & Head
Mechanical Engineering Department
Thapar University, Patiala.

**R.K.SHARMA**
Dean (Academic Affairs)
Thapar University,
Patiala

# ACKNOWLEDGMENT

Working without proper guidance and expecting success is just like making castles in the air, so whenever one wants to start any work, he requires guidance from experts. I express my sincere gratitude to my guide ,Mr. Satish Kumar, lecturer , Department of Mechanical Engineering, Thapar University**,** for acting as supervisor and giving valuable guidance during the course of this investigation, for his ever encouraging and timely moral support. His enormous knowledge and intelligence always helped me unconditionally to solve various problems.

I am greatly thankful to Dr. S. K. Mohapatra, Professor and Head, Mechanical Engineering Department, Thapar University for his encouragement and inspiration for execution of the thesis work. I do not find enough words with which I can express my feeling of thanks to entire faculty and staff of Department of Mechanical Engineering, Thapar University, Patiala for their help, inspiration and moral support, which went a long way in successfully completion of my thesis.

**Karan Rajdev**

# ABSTRACT

Conventional design methods of centrifugal pump are largely based on the application of empirical and semi-empirical rules along with the use of available information in the form of different types of charts and graphs in the existing literature. The program developed in this present work is the best suitable for low specific speed radial centrifugal pump. Same program is also suitable for the design of high specific speed and multistage centrifugal pump with few modifications.

As the design of centrifugal pump involve a large number of interdependent variables, several other alternative designs are possible for same duty. Hence theoretical investigation supported by accurate experimental studies of the flow through the pump.

For the simulation computer program code has been developed which permits wide range of variables to be investigated. A numerical model of an impeller has been successfully generated for calculating pressure distribution of flow fields by using Ansys-CFX code. Simulation results are obtained at blade streamwise location, meridional surface, also stress analysis by using Finite Element Method

# CONTENTS

# LIST OF FIGURES

# NOMENCLATURE

| SYMBOLS | STANDS FOR |
|---|---|
| a | Constant used in determination of the shaft power |
| $A_{th}$ | Throat area at volute in $m^2$ |
| $B_1$ | Impeller width at inlet in m |
| B2 | Impeller width at outlet in m |
| $B_3$ | Inlet width of volute in m |
| Cp | Specific heat |
| D | Diameter in m |
| $D_e$ | Impeller eye diameter in m |
| $D_h$ | Hub diameter in m |
| $D_{sh}$ | Shaft diameter in m |
| dp/r | Mean blade loading |
| f | Weighting factor |
| $f_s$ | Shear stress $N/m^2$ |
| g | Gravitational acceleration in $m/s^2$ |
| H | Head in m |
| $h_1$ | Suction head loss in m |
| $h_2$ | Incidence loss in m |
| $h_3$ | Blade loading loss in m |
| $h_5$ | Mixing loss in m |

| | |
|---|---|
| $h_6$ | Disk friction loss in m |
| $h_7$ | Recirculation loss in m |
| $h_9$ | Internal loss in m |
| $h_L$ | Total loss in head in m |
| $H_d$ | Depression head in m |
| $K_m$ | Capacity constant |
| $N_s$ | Specific speed of pump in rpm |
| N | Speed in rpm |
| $P_{in}$ | Input power in HP |
| $P_{sh}$ | Shaft power in HP |
| Z | Number of blades |
| r | Radius in m |
| $R_t$ | Tongue radius in m |
| $R_e$ | Reynolds number |
| t | Blade thickness in m |
| U | Peripheral velocity in m/s |
| $U_e$ | Peripheral velocity at the eye diameter |
| $V_r$ | Relative velocity in m/s |
| Q | Flow rate in m3/s |
| A | Angle at which the water leaves the impeller |
| β | Blade angle |
| η | Overall efficiency |
| $\theta_A$ | Maximum total angle between the side |

| | |
|---|---|
| | of the volute |
| $\nu$ | Kinematic viscosity $m^2/s$ |
| $\sigma$ | Slip factor |
| $\Psi$ | Head coefficient |
| $\Omega$ | Angular velocity in rad/s |
| $\theta$ | Volute angle |
| $\theta_t$ | Tongue angle |
| $\tau$ | Permissible stress $N/m^2$ |
| $\Phi$ | Flow coefficient |
| $\rho$ | Density of the fluid |
| $g$ | Acceleration due to gravity |

**Subscripts:**

| | |
|---|---|
| 0 | Eye of the Impeller |
| 1 | Inlet to the Impeller |
| 2 | Outlet of the Impeller |
| 3 | Inlet to the Volute |

`

# CHAPTER-1
# INTRODUCTION

## 1.1 Pump

A **pump** is a machine used to move liquid through a piping system and to raise the pressure of the liquid. A pump can be further defined as a machine that uses several energy transformations to increase the pressure of a liquid.

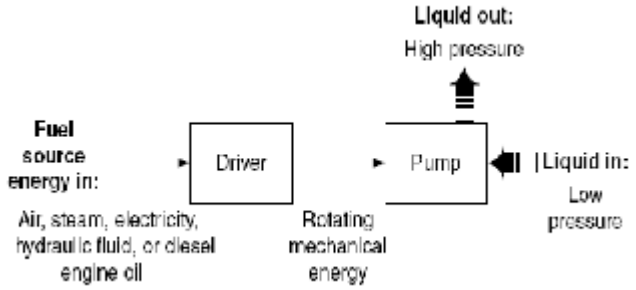


Fig 1.1 Working Principle of Pump

## 1.2 Historical Background

The transfer of liquids against gravity existed from time immemorial. A pump is one such device that expends energy to raise, transport, or compress liquids**.** Pumps are used in a wide range of industrial and residential applications. Pumping equipment is extremely diverse, varying in type, size, and materials of construction. There have been significant new developments in the area of pumping equipment since the early 1980s. Vast tonnages are pumped every year in the form of solid-liquid mixtures, known as slurries. The application which involves the largest quantities is the dredging industry, continually maintaining navigation in harbors and rivers, altering coastlines and winning material for landfill and construction purposes. Dredging is one of the most common and ancient processes involving slurry flows; the dredged materials contain a wide range of particles, tree debris, rocks, etc. Mining has employed the concept of slurry flows in pipelines since the mid-nineteenth century, when the technique was used to reclaim gold from placers in California. Long-distance slurry pipelines have evolved in all continents since the mid 1950s. Some slurry mixtures consist of very fine solids at high concentration; other mixtures are based on coarse particles up to a size of 150 mm.

## 1.3 Classification of Pumps

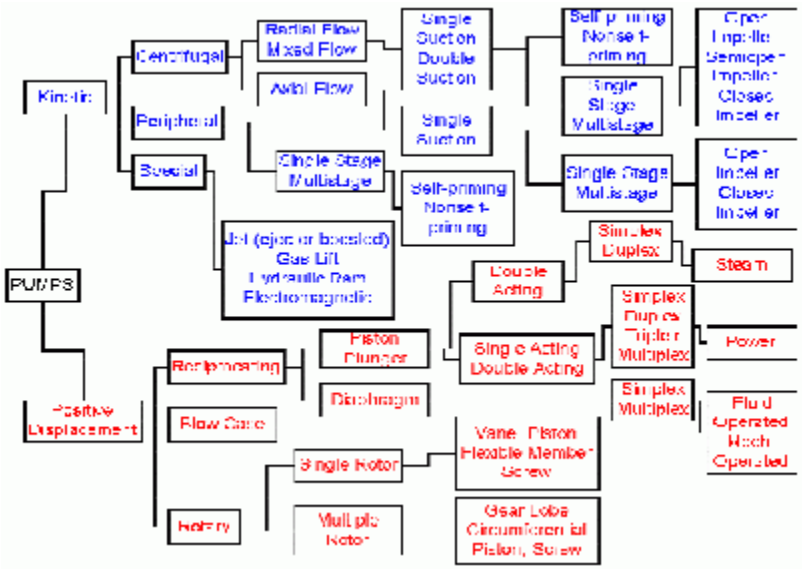


Fig 1.2 Classification of Pump

### 1.3.1 Reciprocating pump

In a positive displacement reciprocating pump, discrete volumes of fluid are isolated between the moving and stationary parts, and moved from the suction to the discharge branch by direct mechanical action. Hence the flow path is not continuous, as it is with a rotodynamic pump. Such pumps necessarily give a pulsating flow, although pulsations can be reduced with multi-cylinder pumps, or by using damping devices

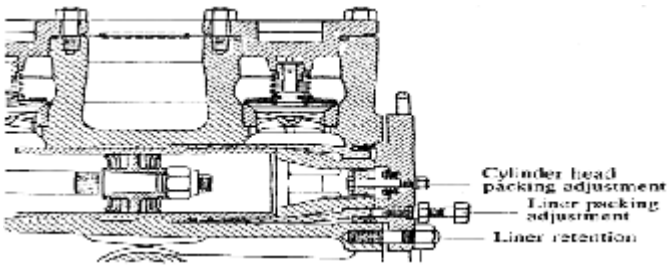


Fig 1.3 Working Principle of Reciprocating pump

### 1.3.2 Rotary Pump

Rotary pump is used to move heavy or very viscous fluids.These employ mechanical means such as gear, cam and screw to move the liquid

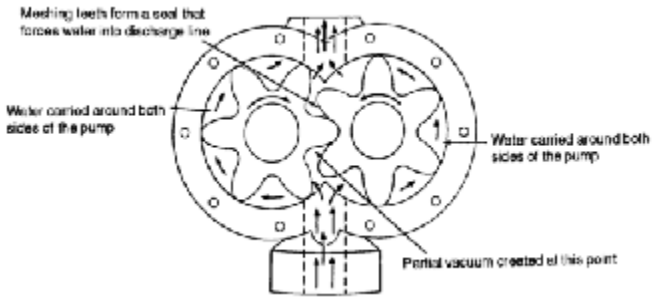


Fig 1.4 Working Principle of Rotary Pump

## 1.4 CENTRIFUGAL PUMPS

The hydraulic machines, which convert the mechanical energy into hydraulic energy, are called pumps. The hydraulic energy is in the form of pressure energy. The mechanical energy is converted into pressure energy by means of centrifugal force acting on the fluid; the hydraulic machines are called centrifugal pumps. The flow in a centrifugal pump is in radial outward direction. Figure 1.4 shows the 3 dimensional model of a centrifugal pump.

### 1.4.1 Working Principle of centrifugal pump

The centrifugal pump works on the principle of forced vortex flow, which means that when a certain mass of liquid is rotated by an external flow, the rise in pressure head of the rotating liquid takes place. The rise in pressure head at any point of the rotating liquid is proportional to the square of tangential velocity of the liquid at that point. Thus at the outlet of the impeller where the radius is more, the rise in pressure head will be more and the liquid will be discharged at the outlet with high pressure head. Due to high-pressure head, the liquid can be lifted to a high level. Figure 1.5 shows flow of fluid in a centrifugal pump.

### 1.4.2 Advantages of using centrifugal pumps for transportation of slurry

1) Simplicity of design
2) Easier installation
3) Low maintenance
4) Lower weight
5) Handles suspensions and slurry easily

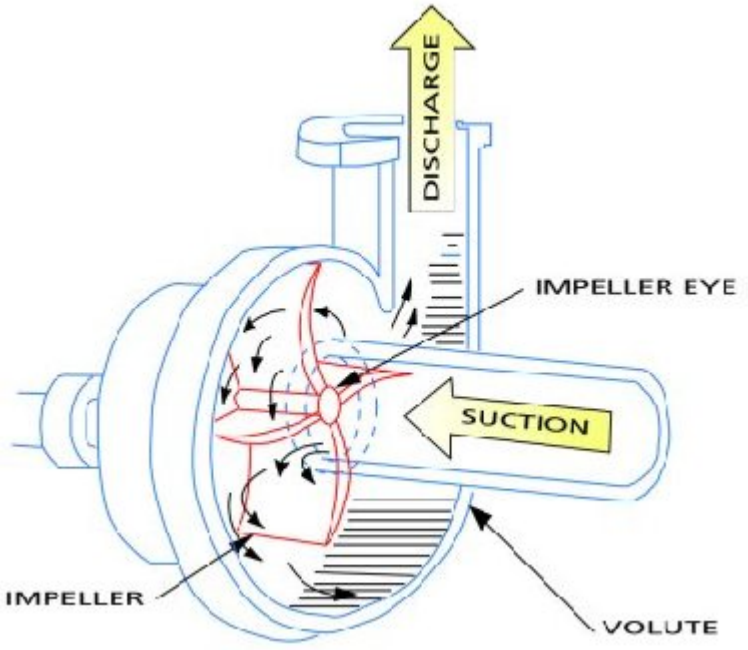


**Figure 1.5 Flow of fluid in a centrifugal pump**

### 1.4.3 Types of centrifugal pumps

Centrifugal pumps can be classified into three general categorized according to the way the impeller imparts energy to the fluid. Each of these categories has a range of specific speeds and appropriate applications.

The three main categories of centrifugal pumps:

1) Radial flow Impellerzz
2) Mixed Flow Impeller
3) Axial flow Impeller

#### 1.4.3.1. Radial flow impeller

Most centrifugal pumps are of radial flow. Radial flow impellers impart energy primarily by centrifugal force. Water enters the hub and flows radically to the periphery. Flow leaves the impeller at 90 degree angle from the direction it enters the pump.

#### 1.4.3.2. Mixed flow impeller

Mixed flow impellers impart energy partially by centrifugal force and partially as an axial compressor. This type of pump has a single inlet impeller with flow entering axially and discharging in an axial and radial direction. Mixed flow impellers are suitable for pumping untreated waste water. They operate at high speeds than the radial flow impeller pumps; are usually of lighter construction; and where applicable, cost less than other pumps. Impeller may be either open or enclosed, but enclosed is preferred.

#### 1.4.3.3. Axial flow impeller

Axial flow impeller imparts energy to the water by acting as axial flow compressors. The axial flow pump has a single inlet impeller with flow entering and exiting along the axis of rotation (along the pump drive shaft). These pumps are used in low head, large capacity applications such as water supplies, irrigation, drainage etc.

### 1.4.4 Main parts of a centrifugal pump

The following are the main parts of centrifugal pumps

1) Impeller
2) Casing
3) Suction pipes with a foot valve and a strainer
4) Delivery pipe

#### 1.4.4.1 Impeller

The rotating part of centrifugal pump is called impeller. It consists of a series of backward curved vanes. The impeller is mounted on a shaft, which is connected to the shaft of an electric motor. An impeller is usually made of iron, steel, aluminium or

plastic, which transfers energy from the motor that drives the pump to the fluid being pumped by forcing the fluid outwards from the centre of rotation. Figure 1.6a shows the axial, radial and tangential component of flow.

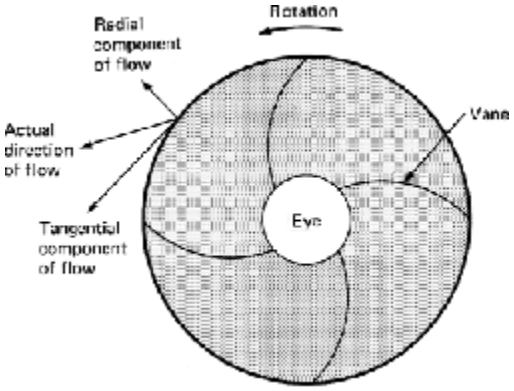


**Figure 1.6a Front view of impeller** **Figure 1.6b 3D model of impeller**

**Components of impeller**

**a) Blade**

Blades are the series of backward or forward curved vanes which transfers the power from shaft to the fluid.

**b) Hub and Shroud**

The hub is the surface of the machine closest to the axis of rotation. It defines the inner fluid flow surface. The shroud is the surface of the machine farthest from the axis of rotation. It defines the outer fluid flow surface. The hub and shroud can be defined only after the machine data has been defined, although all of these objects can be defined in one step.

**c) Leading and trailing edges**

The leading edge curve is the most upstream part of the blade. Any change to the leading edge changes the blade surfaces, which changes the periodic surfaces as well as the hub and shroud surfaces. The trailing edge curve is the most downstream part of the blade.

Impellers are also classified as to whether they are:

**a) Open impellers:**

Most totally open impellers are found on axial flow pumps. This type of impeller would be used in a somewhat conventional appearing pump to perform a chopping,

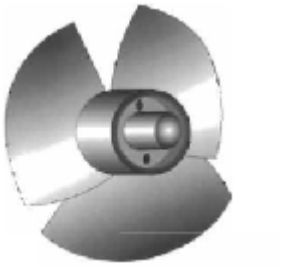

**Figure 1.7 Open Impeller**

grinding action on the liquid. The totally open axial flow impeller moves a lot of volume flow, but not a lot of head or pressure. With its open tolerances for moving and grinding solids, they are generally not high efficiency devices.

**b) Semi-open impeller**

**Figure 1.8 Semi-Open Impeller**

A semi-open impeller has exposed blades, but with a support plate or shroud on one side. These types of impeller are generally used for liquids with a small percentage of solid particles from the bottom of a tank or river, or crystals mixed with the liquid. The efficiency of these impellers is governed by the limited free space or tolerance between the front leading edge of the blades and the internal pump housing wall.

**c) Enclosed impeller**

Totally enclosed impellers are designed with the blades between two support shrouds or plates. These impellers are generally used clean liquids because tolerances are tight at the eye and the housing,and there is no room for suspended solids, crystals or sediment, Figure 1.9. shows a type of enclosed impeller

**Figure 1.9 Enclosed Impeller**

Cavitation damage, play in the bearings, bent shafts and unbalanced rotary assemblies, and any hydraulic side loading on the shaft and impeller assembly.

**1.4.4.2 Casing**

Casing of a pump is an airtight passage surrounding the impeller and is designed in such a way that the kinetic energy of the water discharged at outlet of the impeller is converted into the pressure energy before the water leaves the casing and enters the delivery pipe.

**Types of casing:**

**a) Volute casing**

Volute casing is of spiral type in which area of flow increase gradually. The increase in the area of flow decreases the velocity of flow.The decrease in velocity increases the pressure of the water flowing through the casing. In case of volute casing the efficiency of the pump increase slightly as a large amount of energy is lost due to formation of eddies in this type of casing.

**b) Vortex casing**

If a circular chamber is introduced between the casing and the impeller, the casing is known as vortex casing. By introducing the circular chamber, the loss of energy due to formation of eddies is reduced considerably. Thus, the efficiency of the pump is more than the pump with volute casing.

**c) Casing with guide blades**

In this type of casing, the impeller is surrounded by series of guide blades mounted on a ring, which is known as diffuser. The guide vanes are designed in such a way that water from the impeller enters the guide vanes without stock. Also the area of guide vanes increase, thus reducing the velocity of flow through guide vanes and consequently increasing the pressure of pressure of water. The water from the guide vanes then passes through the surrounding casing, which is concentric with the impeller

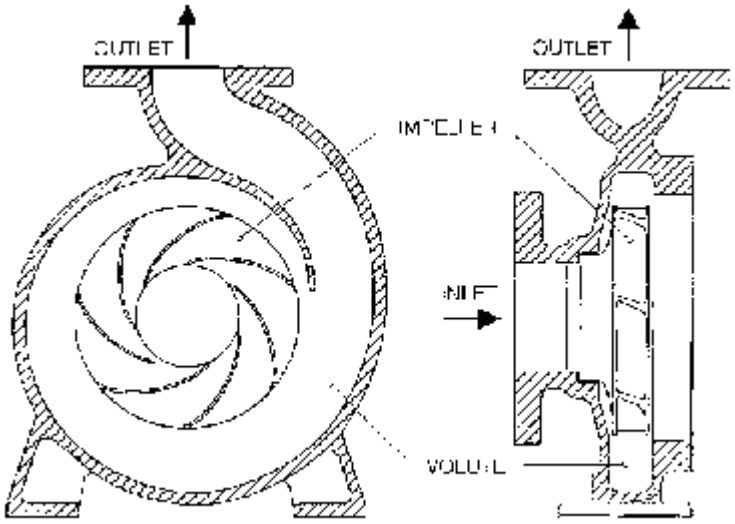


**Figure 1.10 Sectional view of centrifugal pump**

**1.4.4.3 Suction pipe with a foot valve and a strainer**

A pipe whose one end is connected to the inlet of the pump and the other end dips into water in a sump is known as a suction pipe. A foot valve, which is non-return valve or one-way type of valve, is fitted at the lower end of suction pipe. The foot valve opens only in the upward direction. A strainer is also fitted at the lower end of suction pipe

**1.4.4.4 Delivery pipe**

A pipe whose one end is connected to the outlet of the pump and the other delivers the water at the required height is known as delivery pipe.

### 1.4.5 Centrifugal pump applications

Pumps are used wherever any quantity of liquid must be moved from one place to another. Pumps are found in such services as steam power plants; water supply plants; sewage; drainage or irrigation; oil refineries, chemical plants and steel mills; food processing factories and mines; dredging or jetting operations; hydraulic power services and almost every ship whether driven by diesel or steam engine. While these pumps have much in common, they are varied to meet special requirements and particular needs of each service.

- Petroleum Industry
- Chemical Industry
- Textile Industries
- Paper Industry
- Sewage and Sump Services
- Irrigation, Drainage and Flood Control

# CHAPTER-2
# LITERATURE REVIEW

**V P Vasandhani et al[1] [1975]** conducted an experiment using a volute type radial pump with vertically split casing. They observed in the experiment that by changing the length or angle of the tongue of volute, best efficiency point can be shifted to different values of discharge and that the short tongue and a smaller tongue angle give broader efficiency curves without any change in the best efficiency of the pump. They determined the power-discharge, head discharge and efficiency discharge characteristics by setting tongue of volute at seven different positions.

**Jaroslaw mikielewicz et al[2] [1978]** have described a semi empirical method of ideal performance of a centrifugal pump to develop a head loss ratio by examining both single as well as two phase flow. They developed this ratio by dividing loss of head in two phase to loss of head in single phase flow using same values of flow rate and flow coefficient. The techniques used are first, second quadrant operations. In first quadrant, rotation is taken normal and in second quadrant reverse rotation is taken. They found that in both the cases results can be reproduced with acceptable accuracy

**J.W Crisswell[3] [1982]** objective of this paper was to study the problems encountered in the pumping of slurries over short and long distances using centrifugal slurry pump. He discussed the effects of various parameters like friction loss, impeller speed, N.P.S.H, gland sealing in context of problems associated with selection and operation of slurry pump. He showed that wear is the most important factor related to slurry pump selection

**J. Remisz et. al[4] [1983]** have presented a method of transforming pump characteristics from clear water to slurry performance. This permits calculation of the main dimensions of a new slurry pump and also the prediction of the characteristic shape. It has been stated

that changes to the water characteristic depend basically on the type of solid forming the mixture its grain composition, grain geometry, mixture concentration and density..

**W.Mez[5] [1984]** presented the influence of solids concentration, solid density and grain size distribution on the working behaviour of centrifugal pump. In tests 150 mm and 300 mm size pumps with channel type impellers were used. Clean coal, raw coal and gravel were used as slurry having maximum concentration of 40 % by volume and maximum grain size diameter of 125mm.He also compared the results with equations of several authors.

**C I Walker et al[6] [1984]** in this study the change in performance characteristics of centrifugal pumps when handling fine granular or homogeneous type non-Newtonian slurries were examined using two different slurry pumps. Coal/water and kaolin/water was used as slurry. Results showed that the pump performance is dependent on slurry's rheological properties with pump Reynolds number giving generally good correlation with the change in performance

**Koji Kikuyama et al[7][1985]** in this study the changes in the centrifugal pump head and the flow pattern were examined experimentally with use of pump impellers whose outlet edges are deformed stepwise by slicing off the blade on the suction or pressure side. Sharpening of blade caused a change in exit flow angle as well as decrease in velocity and an increase in the pump head was brought about. He presented a simple theory to predict the relationship between increase in pump head and the blade edge sharpening.

**K.K Sheth et al[8] [1987]** carried out experiments to determine the effect of slip factor of slurry pump due to various parameters .Pumps were operated with three different slurries with different speeds. Euler's equation was used to find the equations of slip & friction factors of the flow. Results showed that slip factors deduced from head flow rate curves were more reliable than those deduced from power flow rate curves.

**Rayan and Shawky[9] [1989]** have evaluated erosion wear in the centrifugal slurry pump at different rotational speeds with different solid-liquid concentration by weighing method. They have reported that erosion wear rate increases with flow velocity as well as solid-liquid concentrations.

**Dong et al[10] [1992]** used PDV technique to visualize the flow inside the volute of a centrifugal pump. Neutrally buoyant particles of 30μm mean diameter were used as seed and it was observed that although most of the blade effects occur near the impeller tip, they are not limited to this region.

**V.K Gahlot et al.[11] (1992)** presented the effect of two different types of slurries namely zinc tailing & coal on the performance characteristics of centrifugal slurry pump. A correlation for predicting the reduction head in pump due to slurry flow was proposed. They observed that the head and the efficiency of the pump decrease with increase in solid concentration, particle size and specific gravity of solids where they are independent of the pump flow rate.

**T.Cader et al.[12] (1992)** have investigated water and solid water mixture flow at the impeller outlet of a centrifugal slurry pump using LDV (Laser Doppler Velocimetry) system. Solid particle were taken as 0.8 mm diameter glass beads. They observed that solid particles have larger radial velocity than the carrier fluid at the impeller outlet, but they lag the water in the circumferential direction.

**Cader et al[13] [1994]** have studied phase velocity distribution and overall performance of a centrifugal slurry pump by using LDA (Laser Doppler anemometer).Experiments conducted with a dilute suspension of concentration of 1% micron size tracers and 0.8 mm glass beads at the impeller casing flow interface. They evaluated the liquid and solid velocity distribution in the pump and observed that fluctuations of the pump flow rate, head and loss in efficiency due to particle slip, as the function of impeller position.

**W.Huang et al.[14] [1995]** investigated that two phase flow structure at the impeller-volute interface by using laser doper velocitimetry (LDV).they observed that in the impeller casing slip velocity, solid liquid velocity fluctuations are the function of radial distance and impeller angle. In the impeller rotation region flow is approximately forced vortex type and in casing region free vortex type.

**S.Yedidiah[15] [1996]** discusses the present state of knowledge of the manner in which the impeller geometry affects the developed head. A comparison with test results shows a very impressive agreement between theory and practice.

**S.Yedidiah[16] [1996]** discussed a novel approach for calculating the head developed by a centrifugal impeller. The approach was based on the fact that the head developed by an impeller depends on the shape of the total blade and not just upon the magnitude of its outlet angle. Presented approach was useful in solving many problems encountered with centrifugal pumps.

**Ni et al.[17] (1996)** have experimentally evaluated the effect of high delivered volumetric concentration ($c_{vd}$) on characteristics of a slurry pump. They performed extensive experiments by using three sorts of narrowly graded sands for the observation of pump and pipeline characteristics. They conclude that high solid concentration has a strong influence on the pump head, efficiency and power consumption and this influence behaves differently with different sand size. The pump efficiency in coarse sand slurry service may drop almost 60% compared to that of water service, when $c_{vd}$ = 42%. Within the measured range of concentrations in each passages may experience similar stratification process occurred in pipelines. The mechanical friction regime in the impeller passages could be similar to that in pipelines. Therefore the delivered volumetric concentration and the size affect the head loss in the same way both in pumps and pipelines.

**Miner, S. M. [18] [1997]** has calculated numerically the flow field and pressure field within the rotor of an axial flow pump. Velocity and pressure profiles were developed on both

sides of the impeller. It is observed that the value of tangential velocity increases from the centre line to the outer radius. The axial velocity profile shifts towards the outer radius because of the presence of nose on the hub. The use of coarse and fine mesh does not show significant difference in the values, thus even coarser mesh can be used

**S. Gopalakrishnan[19] [1999]** has discussed the R & D efforts of past, present and future, in terms of core competencies, which are essential for today's pump manufacturer. These are hydraulics, vibrations and pump designs, which capitalize on improved understanding of the underlying technologies.

**Chung[20] [1999]** has developed optimum design code of the pump. They determined the geometric and fluid dynamic variables under the appropriate design constraints. Optimization problem has formulated with a non-linear objective function to minimize losses, net positive suction head required and product price of a pump stage depending on the weighting factor selected as the design compromise. Optimal solution obtained, efficiency $NPSH_R$ depends design variable of centrifugal pump. Selected in the range of weighting factor 0 to 1.designer can easily find the optimum value of design variable to meet their particular requirement of pump design.

**Sellgren et al.[21] (2000)** showed that the addition of clay to sand slurries has been found to reduce the pipeline friction losses, thus lowering the pumping head and power consumption. Pump water heads and efficiencies are decreased by the presence of solid particles. Experimentally results are presented for a centrifugal pump with an impeller diameter of 0.625 m for three narrowly graded sands with average particle sizes of 0.64, 1.27 and 2.2 mm. Reductions in head and efficiency are lowered by about one third for sand clay mixtures with sand to clay mass ratios between 4:1 and 6:1.

**Gandhi et al.[22] [2001]** have studied erosion wear at various locations inside the volute casing of a centrifugal slurry pump for the flow of solid-liquid mixtures. They reported that the wear increases all along the volute periphery with increase in the amount of solid suspended in the mixture and wear smaller when the pump operates near the (BHP).

**Gandhi et al.[23] (2001)** have studied the performance of two centrifugal slurry pumps for three solids materials having different particle size distribution (PSD) in terms of head, capacity and power characteristics. The results have shown that values of head and efficiency ratios are not only depended on solid concentration but are also affected by PSD of the solids and properties of slurry. They conclude that the head and efficiency of the pump decrease with increase in solid concentration, particle size and slurry viscosity, the decrease in the head being 2-10% higher than that of the efficiency. The presence of finer particles (<18 μm) in coarse slurries substantially attenuate the loss of the performance of the pump in terms of head and efficiency

**M C Roco[24] [2001]** has identified qualitative aspects of the flow pattern as large scale periodical, two phase flow structures develop in the entire casing and are dominated by stationary works, particles generally lead the fluid in the radial direction and log in circumferential direction the averaged velocity distribution averaged over the casing width determines the flow rate.

**Oh and Kim[25] [2001**] developed a conceptual design optimization code for mixed flow pump to determine the geometric and fluid dynamic variables under appropriate design constraints. Optimization problem has been formulated with a nonlinear objective function to minimize the fluid dynamics losses.

**Chung M K et al[26] [2001]** developed a simple and accurate correlation for the slip factor of centrifugal impeller. Correlation provided was a function of number of vanes, vanes exit angle & the inlet-exit radius ratio. He investigated the radius of relative eddy inscribed by two adjacent vanes and the exit circle of a flow channel in the impeller to obtain the correlation.

**Engin and Gur[27] [2001]** have studied the effects of different solid-liquid mixture properties on the performance characteristics of a centrifugal enshrouded impeller pump, considering the variation of the tip clearance. The effect of the clearance between the

impeller tip and the casing and of the solid concentration, density and mean diameter on the pump performance characteristics is investigated.

**Stephan Bross et al[28] [2002]** predicted the influence of different design parameters on the wear behaviour of centrifugal slurry pump's impeller suction sealing .For this purpose he developed a simple model and using this model he calculated the velocity field in the impeller suction side and also a comparison was done between analytical solution & numerical solution provided by a CFD package FLUENT.

**Gandhi et al[29] [2002]** have evaluated performance charactereristics of a centrifugal slurry pump at different rotational speeds with water as well as solid-liquid mixture. They found that the affinity relations applicable to conventional pumps for head and capacity can be applied to slurry pumps handling water and slurries at low concentrations (<20% by weight). For higher solids concentrations, these relationships needed to be corrected by taking into account the effect of solids.

**Goto Akira et al[30] [2002]** have proposed a computer aided design system for hydraulic parts of pumps including impellers, bowl diffusers, volutes and vaned return channels. Technologies include 3D-CAD modeling, automatic grid generations, CFD analysis and a 3D inverse design method.

**Egin and Gur[31] [2003]** have evaluated some existing correlations to predict head degradation of centrifugal slurry pumps. A new correlation has been developed in order to predict head reductions of centrifugal pumps when handling slurries. The proposed correlation takes into account the individual effects of particle. The proposed correlation is therefore recommended for the prediction of performance factors of ''small-sized'' slurry pumps having impeller diameters lower than 850 mm size, particle size distribution, specific gravity and concentration of solids, and impeller exit diameter on the pump performance.

**Kadambi et al[32] [2004] )** have used Particle Image Velocimetry to investigate the velocities of the slurry in the impeller of a centrifugal slurry pump for sodium-iodide solution (NaI) and 500micron glass beads slurry. The experiments conducted at 725 rpm, 1000rpm speed, and1%, 2%, 3% volumetric concentration. They observed that the in clear fluid flow conditions for both the pump rpm, flow separation takes place on the suction side of the blade in the region below the blade tip. For the same flow conditions, the flow moves smoothly along the suction side of the blade depicting a recirculation zone. The intensity of this recirculation zone decreases at the higher concentration of 3% due to particle inertia effects. On the pressure side of the blade the particles are pushed along the blade surface and can result in the frictional wear.

**Graeme R. Addie et al[33] [2005]** have discussed numerical model of flow and particles. They have used the experiments which have been conducted to obtain the particle velocities inside an optically transparent acrylic pump using Particle Image Velocity (PIV). They have presented effect of different parameters on operating cost of pump. They concluded that wear parts cost of slurry pumps may be about 50% of the total operating cost of pumps.

**Addie et al.[34] [2007]** have developed ANSI/HI standard of centrifugal slurry pump. They studied the effect of slurry on pump performance; net positive suction head required and wear by using the ANSI/HI standard.

**Pullum et al.[35] [2007]** have calculated the performance reduction of the centrifugal slurry pump by using Hydraulic Institute method for handling non-Newtonian coarse particle suspensions. Suspensions up to 38% v/v of coarse particles with mean diameters in the range of $1.1 < d50 < 3.4$ mm suspended in carrier fluids with dynamic yield stresses of $0 < \tau\gamma < 17.2$ Pa and shear thinning indices in the range $0.35 < n < 0.79$ were examined. They found that the reduction in the head is the function of coarse solid concentration.

**Min-Guan, Y. et al[36] [2007]** have observed the phenomena of two-phase flow with salt crystallizing in the chemical pump, the 3-D turbulent flow in the impeller of chemical

pump was simulated at the condition of rinsing. The internal flow between the impellers of chemical pump was investigated. Based on the Reynolds-averaging N-S equations and the standard $k$-ε two equations turbulent model, the simulations of turbulent flow between the impellers were performed using the flow computing software Fluent under different operating conditions. Based on the analysis of the calculated results of velocity and pressure profiles in the chemical pump and experimentally observed phenomenon of flow impact, secondary flow and recirculation, some design improvements were proposed, which give suggestions on the optimal design and internal two-phase flow study of the chemical pump.

# CHAPTER 3

# DESIGN OFCENTRIFUGAL PUMP

## 3.1 CONVENTIONAL DESIGN OF PUMP:

Conventional design method of centrifugal pump are largely based on the application of empirical and semi-empirical rules along with the use of available information in the form of different types of charts and graphs in the existing literature. The program developed is best suitable for low specific speed centrifugal pump. Same program is also suitable for the design of high specific speed and multistage centrifugal pump with few modifications.

As the design of centrifugal pump involve a large number of interdependent variables, several other alternative designs are possible for same duty. Hence theoretical investigation supported by accurate experimental studies of the flow through the pump. Impeller as it is the element which transfers energy to the fluid stream influences the performance of the pump. Different authors have suggested different design procedure, method of calculation.

The problem of calculation of the dimension of an impeller and hence of the whole pump for given total head may have several solutions but they are not likely to be of equal merit, when considered from the point of view of efficiency and production cost.

Designs suggested by Stenoff has been carefully studied. Each design parameter has been calculated using above procedures and an appropriate value adapt for present carefully analyzing the calculated values.

## 3.2 DESIGN PROBLEM

**INPUT DATA**

Head = 40m  Flow Rate = .080$m^3$/sec

Speed = 1450 rpm

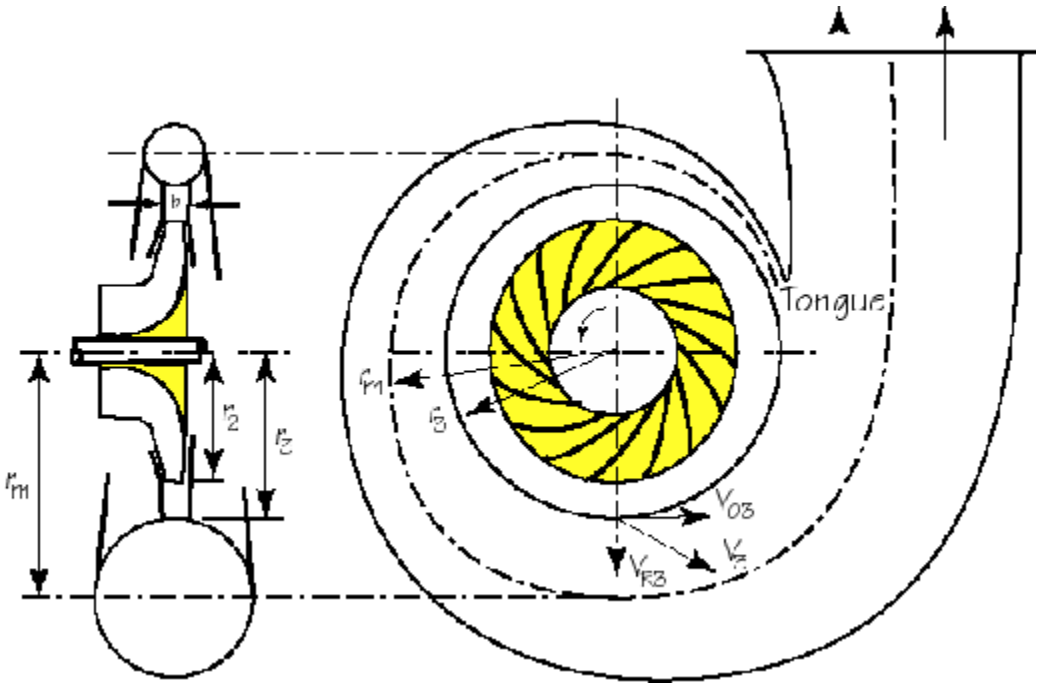


## 3.3 DESIGN OF IMPELLER:

### SPECIFIC SPEED:

Specific speed of the pump is computed based on the power as well as discharge, different authors expressed the design parameter as function of specific speed.

$$\mathbf{Ns = N \sqrt{Q} / H^{3/4}} \qquad \textbf{(3.1)}$$

Where N = speed at pump shaft rotated.

Q = discharge in $m^3$ / sec

H = net head in m.

For given data $N_s = \dfrac{1450x\sqrt{.080}}{(40)^{3/4}} = 25.79\text{rpm}$

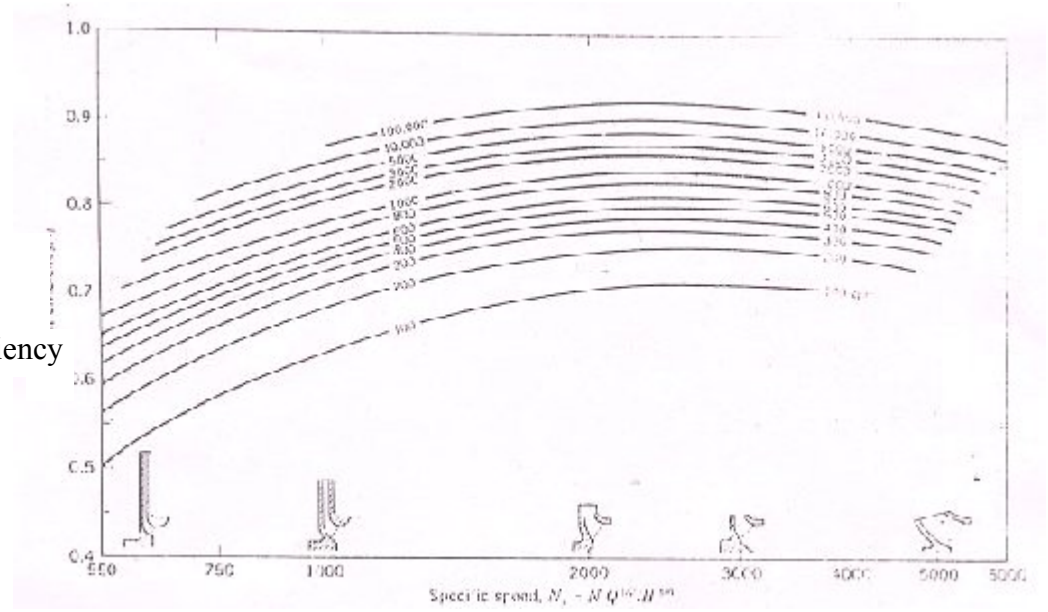


Fig 3.1 Efficiency Vs Specific Speed [37]

## POWER INPUT AND SHAFT INPUT POWER:

$$P_0 = \text{output} = \rho gQH = 1000 * 9.81 * Q * H / 745 \qquad (3.2)$$

Overall efficiency taking by the graph, input power required 15% more because of bearing and transmission loss consider.

$$\text{For given data input power, Pin} = \frac{1000x9.81x.080x40}{745x.78}$$

$$= 57.65 \text{ Hp}$$

So,Input required power = 1.15 Pin

$$\text{Psh} = 1.15 \text{ x } 57.65$$

$$= 65.72 \text{ Hp}$$

## SHAFT DIAMETER:

Torque,

$$T = (P * 60 / 2\Pi N) \text{ N m} \qquad (3.3)$$

$$T = \Pi/16 \text{ Fs } d_{sh}^3 \qquad (3.4)$$

Fs = stress depend the material constant

$$d_{sh} = (16T/\pi Fs)^{1/3}$$

$$\text{for given data } d_{sh} = \left(\frac{16x62.36x735x60}{2x3.14x1450x1.5}\right)$$

$$= 0.042486 \text{ m}$$

**HUB DIAMETER:**

(a) $D_{hb} = D_{sh} + 10$ mm for shaft 20mm diameter.[37]

$D_{hb} = D_{sh} + 20$ mm for shaft upto 100mm diameter.

(b) $D_h = (1.2 \text{ to } 1.3)\ D_{sh}$[37]

for given data $D_{hb} = 1.2 \times .042$

$= .0509$

**OUTLET BLADE VELOCITY ($U_2$):**

Head coefficient

$\varphi$ = pressure head generated / maximum Euler head

$$\varphi = gh / \eta U_2^2 \qquad (3.5)$$

Generally,

$\varphi = 0.5$ to $0.6$

$$U_2^2 = (gh / \eta \varphi)$$

$$U_2 = \sqrt{(gh / \eta \varphi)}$$

For given data $U_2^2 = \left(\frac{9.8 \times 40}{.78 \times .58}\right)$

$= 29.43$ m/sec

**OUTLET DIAMETER ($D_2$):**

$$U_2 = \pi D N / 60 \qquad (3.6)$$

$$D_2 = (60U_2 / \pi N)$$

$$\text{for given data} \quad D_2 = \left(\frac{60x29.436}{3.14x1450}\right)$$

$=0.388$ m

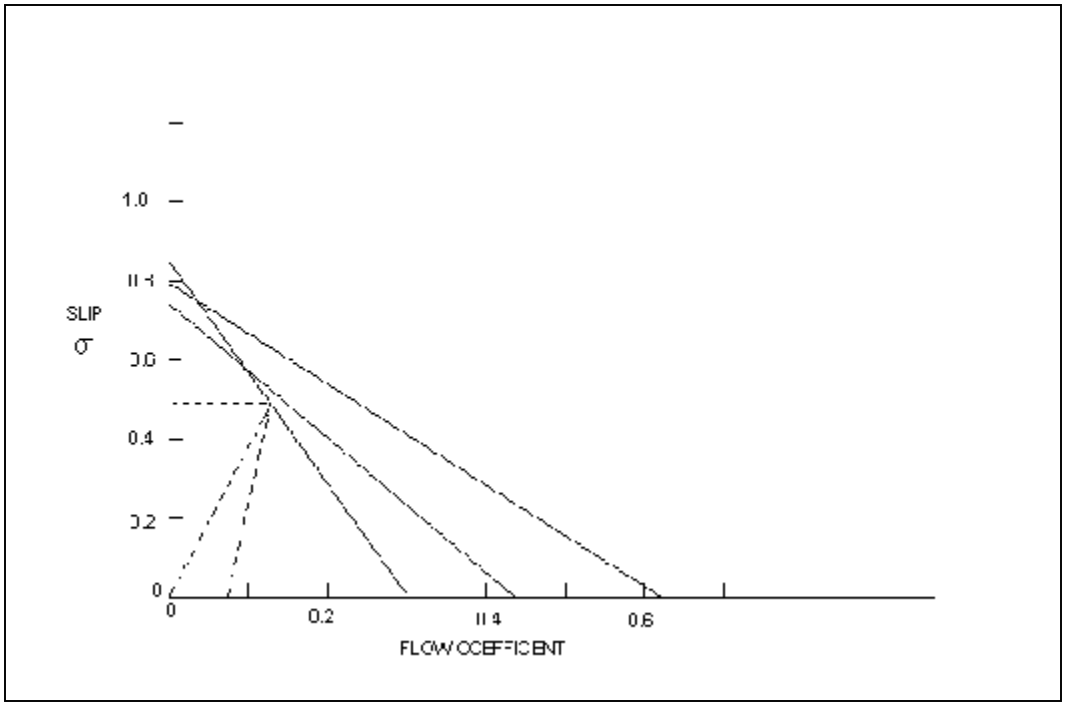


Fig 3.2 **Slip Vs Flow coefficient**[37]

**FLOW COFFICIENT**:

$$\Phi = V_{m2} / U_2 = \text{Flow velocity / Blade velocity} \qquad (3.7)$$

$\Phi$ taken 0.1 to 0.2[37]

$$V_{m2} = \Phi U_2$$

Mean meridional velocity of the steam just after entering the blade passage is denoted by $V_{m1}$ and $V_{m0}$ is the mean meridional velocity of steam just prior to blade inlet. $V_{m2}$ denotes the meridional velocity at the exit of the impeller. Ratio of $\sqrt{2gh}$ is known as capacity constant.

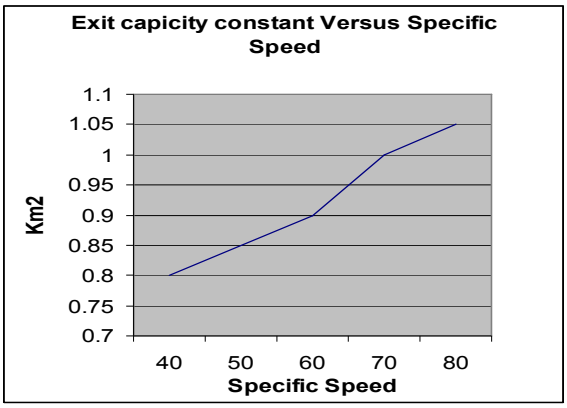


**Fig 3.3(a)**

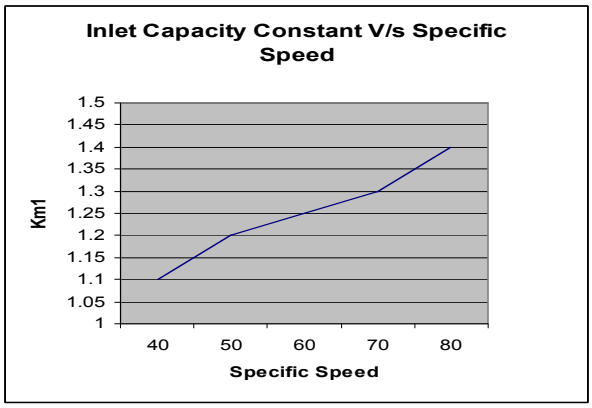


**Fig.3.3(b)**

$$K_{m1} = V_{m1} / \sqrt{2gH}$$

$$K_{m2} = V_{m2} / \sqrt{2gH}$$

To calculate $C_{m1.}$

$$V_{m0} = (0.8 \text{ to } 0.9)\ V_{m1}$$

Stepanoff recommended computation of $V_{m0}$ and $V_{m1}$

$$V_{m0} = (1.3 \text{ to } 1.5)V_{m2.}$$

For given data $V_{m1}$ = .175 x 29.44

= 5.15m/sec

$V_{m2}$ = 1.15 x 5.92

= 5.924 m/sec

**IMPELLER EYE DIAMETER ($D_E$):**

$$Л / 4( D_E^2 - D_H^2 ) V_{m1} = Q \text{ (Flow rate)}$$

$$D_e = [ 4Q / ЛV_{m1} + D_h^2 ]^{1/2}$$

$$D_e^2 = \left[.091^2 + .050^2\right]$$

$$= 0.149 \text{ m}$$

**INLET DIAMETER ($D_1$):**

Stepanoff used the following relationship

$$D_1 = (D_e + 0.020) \text{ m}$$

For given data $D_1 = 0.149 + .020 = 0.1696$ m

**INLET BLADE VELOCITY ($U_1$):**

$$U_1 = (Л D_1 N / 60)$$

For given data $U_1 = \left(\frac{3.14x.1696x1450}{60}\right)$

$$= 12.87 \text{ m/sec}$$

**INLET BLADE ANGLE ($B_1$):**

Fluid at inlet assumed no pressure whirl

$$\beta_1 = \tan^{-1}\left(\frac{V_{m1}}{U_1}\right)$$

for given data $\beta_1 = \tan^{-1}\left(\frac{5.15}{12.87}\right)$

$= 21.82$

Thickness of the blade is mostly taken leading and trailing tips are 4 mm and 5 mm, respectively.

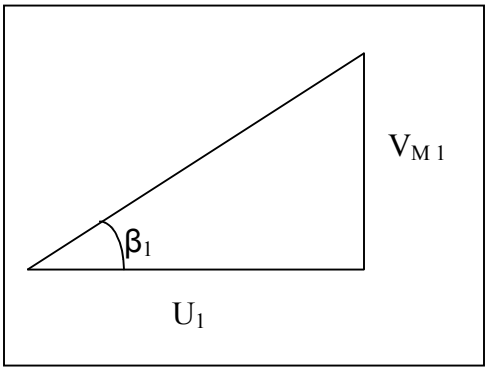


Fig. 3.4 Inlet velocity triangle

**WIDTH OF IMPELLER (B):**

Flow rate (Q) = $(\pi D_2 B_2) \cdot \phi \cdot u_2$

$$B_2 = \frac{Q}{(\pi \cdot D_2 \cdot u_2 \cdot \phi)}$$

$$B_2 = \frac{0.080}{(\pi x.388x29.43x.175)}$$

$= 0.011$ m

**BLADE ANGLE AT OUTLET ($B_2$):**

Stepanoff recommends the equation

$$H = \frac{u_2^2}{g} - \frac{u_2 V_{m2}}{g \cdot \tan B_2'}$$

$B_2' = 1.4 \times B_2$

Assuming the fluid stream is entering the impeller without pre rotation and circulation is zero.

Stepanoff recommended

$$\Psi = \sigma - \Phi \tan\beta_2$$

for given data $40 = \frac{29.43^2}{g} - \frac{29.43x5.92}{g \cdot \tan B_2'}$

$$B_2 = 24.58$$

**NUMBER OF BLADES (Z):**

Number of blades generally taken between 5 to 12.

According to Stepanoff $Z = (B_2 / 3)$.

For given data $Z = (24.58/3)$

$= 8.2$

**OUTLET BLADE TRIANGLE:**

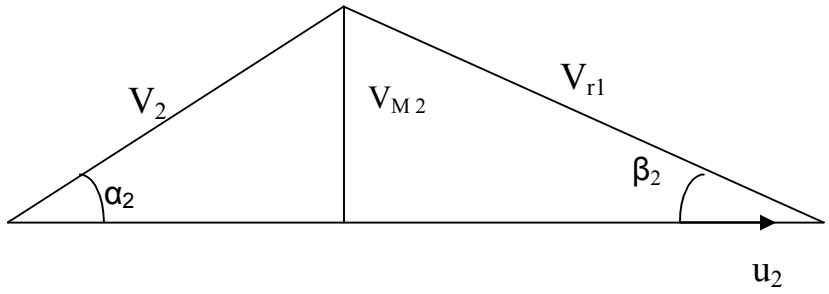


**Fig. 3.5**

From inlet velocity triangle

$V_1 = V_{m1} = 5.15$

$V_{r1}^2 = U_1^2 + V_{m1}^2$

$= 5.15^2 + 12.87^2$

$= 13.86$ m/sec

$V_{rui} = U_1 = 12.87$ m/sec

From outlet velocity triangle

$V_{r2} = V_{m2}/\sin\beta_2$

$= 5.92/\sin 24.58 \quad = 11.28$ m/sec

## 3.4 DESIGN OF VOLUTE CASING:

### 3.4.1 INTRODUCTION:

The objective of the volute is to convert kinetic energy imparted to the liquid by impeller into pressure. Casing has no part in the dynamic generation of total head, it deals only with minimization of losses.

Following element are used to reduce the velocity and kinetic energy:

- Volute casing
- Vane less guide ring.
- Diffuser ring vanes.

Main advantage of volute casing as compared with a casing having diffuser vane is its mechanical simplicity, low cost and ease of manufacture. However the casing with diffuser vane is more efficient than volute casing. Volute casing are preferred for single stage pump and in case of multistage pumps diffuser ring is preferred.

### 3.4.2 DESIGN OF VOLUTE CASING:

Volute casing consists of a casing with gradually increasing area, tongue and a conical discharge nozzle. A circle centered on the axis of rotation and tangent to the volute called the base circle diameter. When rate of flow below the design value some flow return into the volute, passing impeller and tongue through the volute throat, a space between the impeller and tongue must be make small.

Water in the volute has very nearly the spiral flow so that

$$R.V_u = \text{constant.}$$

Let Φ represents the angular distance of any cross-section measured from volute tongue and R is inside radius, r is the radius of elementary strip. Within cross section considered, b is the axial width

Area of elemental ring

$$dA = bdR$$

Discharge through this ring

$$(dQ)_\Phi = dA.\ V_u = b.dR.V_u$$

$$(dQ)_\Phi = bdr / r\ .$$

Total discharge through the cross section is obtained by integrating the equation.

$$Q_\Phi = K \int_{r=r}^{r=R} (b/r)dr$$

Total Q discharge from the pump will be collected in the volute. When more angular distance of 360° from volute tongue.

Discharge at any volute section Φ

$$Q_\Phi = (\Phi/360).Q$$

$$\Phi(\text{degree}) = 360K/Q \int_{r=r}^{r=R} (b/r)dr$$

$$= 360\ R_2\ Cu_2 / Q\ K \int_{r=r1}^{r=R} (b/r)dr$$

Max total angle Qa, between the sides, about 60°. If more water is unable to flow the side hence turbulence and insufficiency result. Qa small and radius large give better result but casing diameter and weight of the pump are increased.

To avoid shock losses the tongue angle should be made the same as absolute outlet angle $\alpha_2$, water leaving the impeller, radius Rt is the 5 to 10% greater than outside radius of impeller to avoid turbulence and noisiness.

Zero point of the volute or point from angle is measured may be found by assuming that flow follows a logarithmic spiral

$$R = R_2\ e^{\tan\alpha 2.\theta}$$

$\Phi$ = Angle in radians

**Throat Angle**

Angle at which the throat of the volute start

Throat angle $Qt = [ \ln (Rt / R_2 ) / \tan \alpha_2$

In order to avoid turbulence total divergence in this passage should not exceed 10°.

**Inlet width of volute**

$B_3 / B_2 = 1.4$ TO 1.8 (for high Ns)

$= 2$ (for low Ns)

**Diameter of Inlet at Volute**

$D_3 = 1.1$ to $1.2 D_2$

**Width of volute at any point**

$$B = B_3 + 2 X \tan (Q_A / 2)$$

$Q_A$ = Taken 60°

X = Distance between any radius R and impeller outside radius

$$R2 = (Rav - R2)$$

Velocity at throat $V_{th} = (D_2 \times V_{u2})/D_3$

For given design problem

### 3.4.3 VOLUTE DESIGN CALCULATION

Inlet Width of Volute $B_3 = 1.8 B_2$

$= 1.8 \times 0.11087$

$= 0.0199$ m

Dia. Of Inlet at Volute

$$D_3 = 1.15D_2$$

$$= 1.15 \times 0.387$$

$$= 0.446 \text{ m}$$

$$R_v = \left( \frac{D_2 + D_3}{4} \right)$$

$$= \left( \frac{0.387 + 0.4461}{4} \right)$$

$$= 0.2085$$

Width at x distance $B_x = B_3 + \left( \frac{2R_v - D_2}{1.73} \right)$

$$= 0.0199 + \left( \frac{2x0.20854 - 0.388}{1.73} \right)$$

$$= 0.0367 \text{ m}$$

Whirl component of velocity at volute

$$V_{u3} = V_2 \cos \alpha_3$$

$$= 5.99 \cos 8.29$$

$$= 1.623 \text{ m/sec}$$

Throat angle Qt = [ ln (0.223 / 0.196 ) / tan 8.29

$$= 38.56^o$$

Velocity at throat $V_{th}$ = (0.387 x 39.03)/0.448

$$= 33.94 \text{ m/sec}$$

# CHAPTER-4
# COMPUTATIONAL FLUID DYNAMICS

## 4.1 Introduction

Computational Fluid Dynamics (CFD) is the analysis of systems involving fluid flow, heat transfer and associated phenomena such as chemical reactions by means of computer-based simulation. The heat and mass transfer, fluid flow, chemical reaction, and other related processes that occur in engineering equipment, in the natural environment, and in living organisms play a vital role in a great variety of practical situations. Nearly all methods of power production involve fluid flow and heat transfer as essential processes. The same processes govern the heating and air conditioning of buildings. Major segments of the chemical and metallurgical industries use components such as furnaces, heat exchangers, condensers, and reactors, where thermo-fluid processes are at work. Aircraft and rockets owe their functioning to fluid flow, heat transfer, and chemical reaction. In the design of electrical machinery and electronic circuits, heat transfer is often the limiting factor. The pollution of the natural environment is largely caused by heat and mass transfer, and so are storms, floods, and fires. In the face of changing weather conditions, the human body resorts to heat and mass transfer for its temperature control. The processes of heat transfer and fluid flow seem to pervade all aspects of our life. Since the above processes have such an overwhelming impact on human life, we should be able to deal with them effectively. This ability can result from an understanding of the nature of the processes and from methodology with which to predict them quantitatively. The designer of an engineering device can ensure the desired performance, if the power of prediction enables him. Predictions of the relevant processes help us in forecasting, and even controlling, potential dangers such as floods, tides, and fires. In all these cases, predictions offer economic benefits and contribute to human well-being. The prediction of behavior in a given physical situation consists of the values of the relevant variables governing the processes of interest. Let us consider a particular example. In a combustion chamber of a certain description, a complete prediction should give us the values of velocity, pressure, temperature, concentrations of the relevant

cherI1ical species, etc., throughout the domain of interest; it should also provide the shear stresses, heat fluxes, and mass flow rates at the confining walls of the combustion chamber. The prediction should state how any of these quantities would change in response to proposed changes in geometry, flow rates, fluid properties, etc

## 4.2 The Position of CFD in the world of virtual Prototyping

To situate the role and importance of CFD in our contemporary technological world, it might be of interest to take you down the road to the global world of Computer-Assisted Engineering or CAE. CAE refers to the ensemble of simulation tools that support the work of the engineer between the initial design phase and the final definition of the manufacturing process. The industrial production process is indeed subjected to an accelerated evolution toward the computerization of the whole production cycle,using various software tools.The most important of them are: Computer-Assisted Design (CAD), Computer-Assisted Engineering (CAE) and Computer-Assisted Manufacturing (CAM) software.The CAD/CAE/CAM software systems form the basis for the different phases of the virtual prototyping environment .The chart presents the different components of a computer-oriented environment,as used in industry to create, or modify toward better properties, a product.

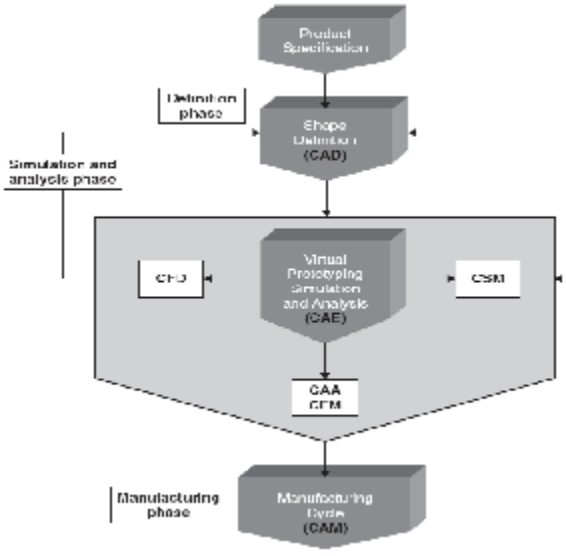


Fig 4.1 Position of CFD in World of virtual Prototyping

## 4.3 How CFD works

Fluid flows and related phenomena can be described by partial differential (or integro-differential) equations, which cannot be solved analytically except in few special cases. To obtain an approximate solution numerically, we have to use a discretization method which approximates the differential equations by a system of algebraic equations, which can then be solved on a computer. The approximations are applied to small domains in space and/or time so the numerical solution provides results at discrete locations in space and time.Much as the accuracy of experimental data depends on the quality of the tools used, the accuracy of numerical solutions is dependent on the quality of discretizations used.CFD is finding its way into process, chemical, civil, and environmental engineering. Optimization in these areas can produce large savings in equipment and energy costs and in reduction of environmental pollution.

## 4.4 Components of CFD simulation

### 4.4.1 Mathematical Model

The starting point of any numerical method is the mathematical model, i.e. the set of partial differential or integro-differential equations and boundary conditions. One chooses an appropriate model for the target application (incompressible, inviscid, turbulent; two- or threedimensional,etc.). The numerical model may include simplifications of the exact conservation laws. A solution method is usually designed for a particular set of equations. Trying to produce a general purpose solution method, i.e. one which is applicable to all flows, is impractical, if not impossible and, as with most general purpose tools, they are usually not optimum for anyone application.

### 4.4.2 Discretization Method

After selecting the mathematical model, one has to choose a suitable discretization method, i.e. a method of approximating the differential equations by a system of algebraic equations for the variables at some set of discrete locations in space and time. There are many approaches, but the most important of which are: finite difference (FD), finite volume (FV) and finite element (FE) methods.Each type of method yields the same

solution if the grid is very fine. However, some methods are more suitable to some classes of problems than others. The preference is often determined by the attitude of the developer.

### 4.4.3 Coordinate and Basis Vector Systems

The conservation equations can be written in many different forms, depending on the coordinate system and the basis vectors used. For example one can select cartesian,cylindrical, spherical, curvilinear orthogonal or non-orthogonal coordinate systems, which may be fixed or moving. The choice depends on the target flow, and may influence the discretization method and grid type to be used.

### 4.4.4 Numerical Grid

The discrete locations at which the variables are to be calculated are defined by the numerical grid which is essentially a discrete representation of the geometric domain on which the problem is to be solved. It divides the solution domain into a finite number of sub-domains (elements, control volumes etc.). Some of the options available are the following:

#### 4.4.4.1 Structured (regular) grid

Regular or structured grids consist of families of grid lines with the property that members of a single family do not cross each other and cross each member of the other families only once. This allows the lines of a given set to be numbered consecutively. The position of any grid point (or control volume) within the domain is uniquely identified by a set of two (in 2D) or three (in 3D) indices, e.g. (i,j, k).This is the simplest grid structure, since it is logically equivalent to a Cartesian grid. Each point has four nearest neighbors in two dimensions and six in three dimensions; one of the indices of each neighbor of point P (indices i,j, k) differs by ±1 from the corresponding index of P. This neighbor connectivity simplifies programming and the matrix of the algebraic equation system has a regular structure, which can be exploited in developing a solution technique. The disadvantage of structured grids is that they can be used only for geometrically simple solution domains.Another disadvantage is that it may be difficult to

control the distribution of the grid points:concentration of points in one region for reasons of accuracy produces unnecessarily small spacing in other parts of the solution domain and a waste of resources. This problem is exaggerated in 3D problems. The long thin cells may also affect the convergence adversely.

Structured grids may be of H, 0, or C type; the names are derived from the shapes of the grid lines.

**a) H-type grid**

Which, when mapped onto a rectangle, has distinct east, west, north, and south boundaries.

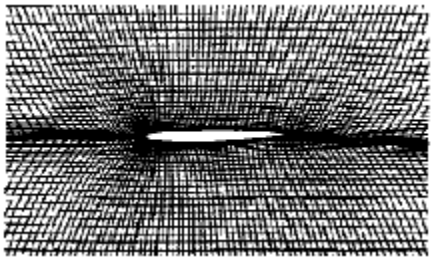

Fig 4.2 H-type grid

**b) O-type grid**

In this type of grid, one set of grid lines is "endless"; if the grid lines are treated as coordinate lines and we follow the coordinate around the cylinder, it will continuously increase and, to avoid a problem, one must introduce an artificial "cut" at which the coordinate jumps from a finite value to zero. At the cut, the grid can be "unwrapped" but the neighboring points must be treated as interior grid points, in contrast to the treatment applied at the boundaries of an H-type grid.

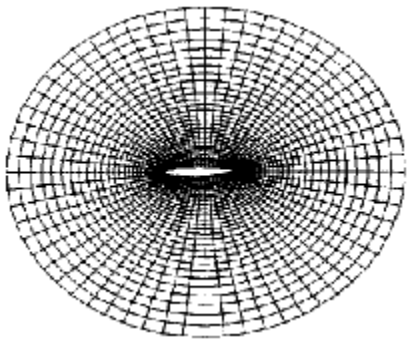

Fig 4.3 O-type grid

**c) C-type grid**

In this type of grid, points on portions of one grid line coincide, requiring the introduction of a cut similar to the ones found in atype grids. This type of grid is often used for bodies with sharp edges for which they are capable of good grid quality.

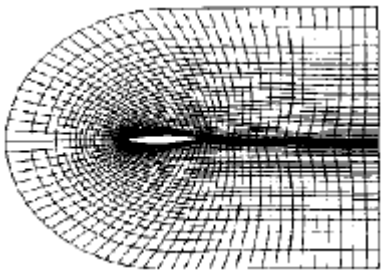

Fig 4.4 C-type grid

**4.4.4.2 Unstructured grids**

For very complex geometries, the most flexible type of grid is one which can fit an arbitrary solution domain boundary. In principle, such grids could be used with any discretization scheme, but they are best adapted to the finite volume and finite element approaches. The elements or control volumes may have any shape; nor is there a restriction on the number of neighbor elements or nodes. In practice, grids made of triangles or quadrilaterals in 2D, and tetrahedra or hexahedra in 3D are most often used.Such grids can be generated automatically by existing algorithms. If desired, the grid can be made orthogonal, the aspect ratio is easily controlled, and the grid may be easily locally refined. The advantage of flexibility is offset by the disadvantage of the irregularity of the data structure. Node locations and neighbor connections need be specified explicitly. The matrix of the algebraic equation system no longer has regular, diagonal structure; the band width needs to be reduced by reordering of the points. The solvers for the algebraic equation systems are usually slower than those for regular grids.

Unstructured grids are usually used with finite element methods and, increasingly, with finite volume methods. Computer codes for unstructured grids are more flexible. They need not be changed when the grid is locally refined, or when elements or control volumes of different shapes are used. However, grid generation and pre-processing are usually much more difficult. An example of an unstructured grid is shown in Fig.

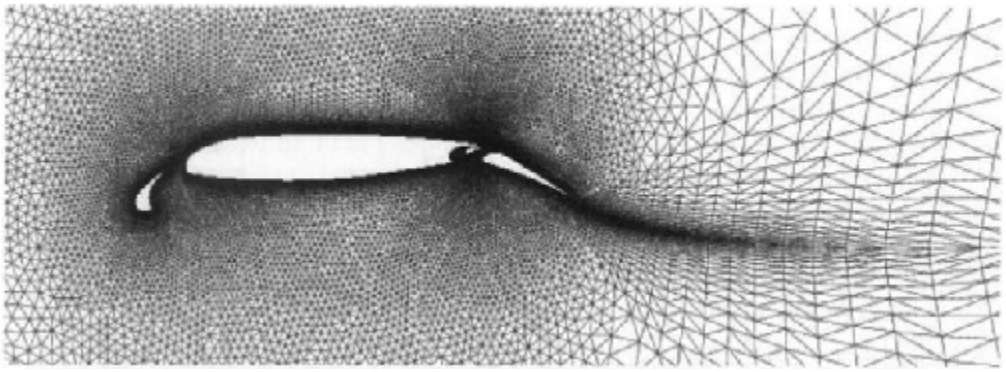

Fig 4.5 Unstructured grid

### 4.4.5 Finite Approximations

Following the choice of grid type, one has to select the approximations to be used in the discretization process. In a finite difference method, approximations for the derivatives at the grid points have to be selected. In a finite volume method, one has to select the methods of approximating surface and volume integrals. In a finite element method, one has to choose the shape functions (elements) and weighting functions.The choice of approximation scheme influences the accuracy of the results. It also affects the difficulty of developing the solution method, coding it, debugging it, and the speed of the code. More accurate approximations involve more nodes and give fuller coefficient matrices.

### 4.4.6 Solution Method

Discretization yields a large system of non-linear algebraic equations. The method of solution depends on the problem. For unsteady flows, methods based on those used for initial value problems for ordinary differential equations (marching in time) are used. At each time step an elliptic problem has to be solved. Steady flow problems are usually solved by pseudo-time marching or an equivalent iteration scheme. Since the equations are non-linear, an iteration scheme is used to solve them. These methods use successive linearization of the equations and the resulting linear systems are almost always solved by iterative techniques. The choice of solver depends on the grid type and the number of nodes involved in each algebraic equation.

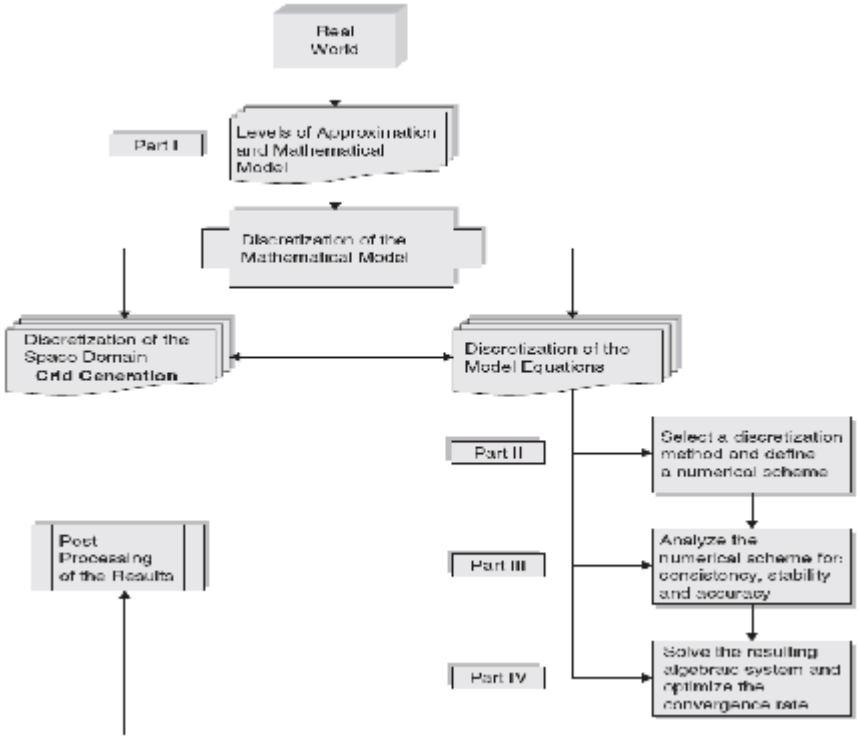


Fig 4.6 Structure of a CFD simulation system.

## 4.5 Errors involved in CFD

Error is a recognizable deficiency in a CFD model that is not caused by lack of knowledge. Cause of errors are:

(a) Numerical errors – round off errors, iterative convergence errors, discretization errors.

(b) Coding errors: mistakes or 'bugs' in the software

(c) User errors- human errors through incorrect use of software. Can be reduced / eliminated through adequate training and experience.

## 4.6 GOVERNIG EQUATIONS OF FLUID FLOW

The physical aspects of any fluid flow are governed by the following three fundamental principles:

a) Conservation of mass
b) Conservation of momentum ( Newton's second law)
c) Conservation of energy ( first law of thermodynamics)

These fundamental principles can be expressed in terms of mathematical equations which in their most general form are usually partial differential equations.cfd is a art of replacing the governing partial differential equations of fluid flow with numbers and

advancing these numbers in space and / or time domain to obtain a final description of complete flow field of interest.with the advent of high-speed digital computers,cfd has become a powerful tool to predict flow characteristics in varied problem,in an economical way.

### 4.6.1 The mass conservation equation

The law of mass conservation is a general statement of kinematic nature, i.e. independent of the nature of the fluid or of the forces acting on it. It expresses the empirical fact that in a fluid system, mass cannot disappear from the system, nor be created. The quantity *U* is, in this case, the specific mass, $U = \rho$ in kg/m3.As noted , no diffusive flux exists for the mass transport, which means that mass can only be transported through convection. With the convective flux defined by *F*C $= \rho\_v$ and in absence of external mass sources, the general integral mass conservation equation then becomes

In differential form

This equation is also called the continuity equation

$$\frac{\partial \rho}{\partial t} + \nabla.(\rho \vec{v}) = S_m$$

The source $S_m$ is the mass added to the continuous phase from the dispersed second phase(e.g. due to vaporization of liquid droplets) and any user-defined sources.

For Steady state compressible fluid flow the continuity equation is given by;

$$\rho\left(\nabla.\vec{v}\right) = 0$$

Where, $\nabla = \frac{\partial}{\partial x_i}\hat{i} + \frac{\partial}{\partial x_j}\hat{j} + \frac{\partial}{\partial x_k}\hat{k}$

And $\vec{v} = u_i \hat{i} + u_j \hat{j} + u_k \hat{k}$

### 4.6.2 Conservation of Momentum

Conservation of momentum in an inertial (non-accelerating) reference frame is described as

$$\frac{\partial}{\partial t}\left(\rho \vec{v}\right) + \nabla.\left(\rho \overleftrightarrow{vv}\right) = -\nabla p + \nabla.\overline{\overline{(\tau)}} + \rho\overline{(g)} + \overline{F}$$

Where $\rho\overline{(g)}$=Gravitational body force

F=external body forces(e.g that arise from interaction with the dispersed phase),respectively.F also contains other model-dependent source terms such as porous-media and user-defined sources.

The stress tensor $\tau$ is given by

$$\bar{\bar{\tau}} = \mu\left[\left(\nabla\bar{v} + \nabla\overline{v^T}\right) - \frac{2}{3}\nabla.\bar{v}I\right]$$

Where the second term on the right hand side is taken for considering the effect of volume dilation.

For steady state incompressible fluid flow,the momentum conservation equation is given by

$$\nabla.\left(\rho\overleftrightarrow{vv}\right) = -\nabla p + \nabla.\left(\bar{\bar{\tau}}\right) + \rho\bar{g} + F$$

**4.6.3 Conservation of Energy**

First law of thermodynamics applied to closed process, i.e. system taken through a complete cycle

$$\int( dQ - dW ) = 0$$

Change in internal energy during change in state from one point to another in the cycle

$$dE = dQ - dW$$

For a steady flow process the conservation of energy per unit time is regarded, i.e. conservation of power. . . . .

$$dE = m\,.\,( dh_0 + g.dZ ) = Q - W$$

Where $dh_0$ denotes the change in total enthalpy and the term g.dZ change in specific potential energy. Apart from hydraulic machines the latter can be neglected. Further more the process can be assumed as adiabatic leading to the conservation of energy for

A steady turbomachine being written as

$$\dot{W} = \dot{m}.( h_{01} - h_{02} )$$

For work absorbing machines ( compressors, pumps) $h_{01} < h_{02} \Rightarrow W < 0$

### 4.7 The k-epsilon model

One of the most prominent turbulence models, the $k-\varepsilon$ ($k$-epsilon) model, has been implemented in most general purpose CFD codes and is considered the industry standard model. It has proven to be stable and numerically robust and has a well established regime of predictive capability. For general purpose simulations, the model offers a good compromise in terms of accuracy and robustness.

Within ANSYS CFX, the $k-\varepsilon$ turbulence model uses the scalable wall-function approach to improve robustness and accuracy when the near-wall mesh is very fine. The scalable wall functions allow solution on arbitrarily fine near wall grids, which is a significant improvement over standard wall functions. While standard two-equation models, such as the model, provide good predictions for many flows of engineering interest $k$ is the turbulence kinetic energy and is defined as the variance of the fluctuations in velocity. It has dimensions of ($L^2T^{-2}$) $m^2/s^2$. $\varepsilon$ is the turbulence eddy dissipation (the rate at which the velocity fluctuations dissipate), and has dimensions of per unit time ($L^2T^{-3}$). The k- model introduces two new variables into the system of equations. The continuity equation is then:

$$\frac{\partial \rho}{\partial t} + \nabla \bullet (\rho U) = 0$$

and the momentum equation becomes

$$\frac{\partial \rho U}{\partial t} + \nabla \bullet (\rho U \otimes U) - \nabla \bullet (\mu_{eff} \nabla U) = -\nabla p' + \nabla \bullet (\mu_{eff} \nabla U)^T + B$$

where

$B$ is the sum of body forces,

$\mu_{eff}$ is the effective viscosity accounting for turbulence,

$p'$ the modified pressure.

mo

### 4.8 Simulation in Ansys CFX

Simulation of fluid flow inside a impeller of mixed flow centrifugal pump was carried out using Ansys CFX tool which is a CFD tool

### 4.8.1 Modelling Impeller

Impeller of centrifugal pump was modelled using Ansys Blade modeler tool. The Blade Modeler software is a specialized, easy-to-use tool for the rapid 3-D design of rotating machinery components. The software can be used to design axial, mixed-flow and radial blade components in applications such as pumps, compressors, fans, blowers, turbines, expanders, turbochargers, inducers and others. BladeModeler provides the essential link between blade design and advanced simulation including computational fluid dynamics and stress analyses.

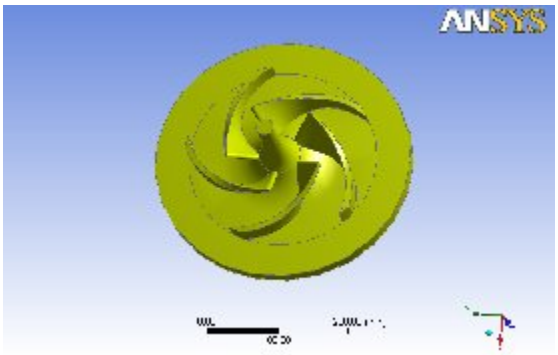


Fig. 4.7 Modeling of Impeller

### 4.8.2 Mesh Generation of Impeller using Turbogrid

Modelled created in first step is than exported to Ansys Turbogrid. ANSYS TurboGrid is a powerful tool that lets designers rotating machinery create high-quality hexahedral meshes, while preserving the underlying geometry. These meshes are used in the ANSYS workflow to solve complex blade passage problems.For this problem , the H/J/C/L-Grid topology was used.O-Grid width factor was taken as 0.2.After that modifications of control points was done on Hub and Shroud because there was error in minimum face angle which was below the minimum described that is 20 degree.So to rectify this problem control points were moved in direction of arrows as shown in figures.This resulted in lowering of errors.

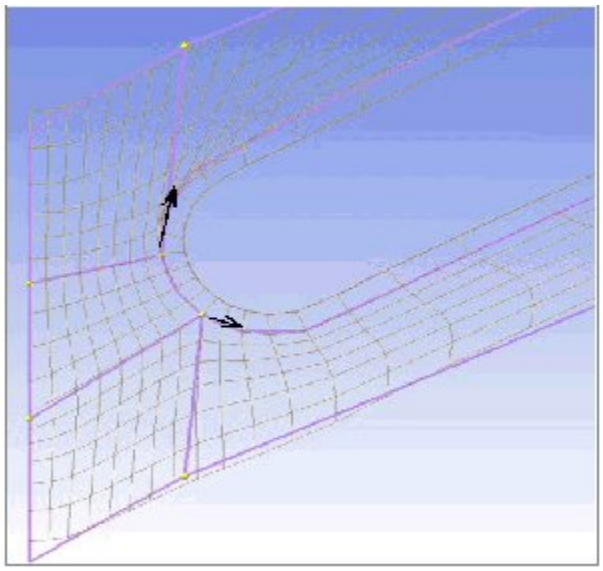

Fig 4.8 Modifying Control Points on the Hub

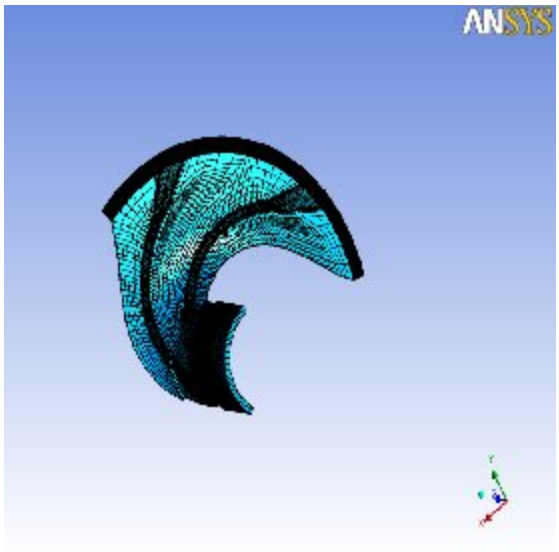


Fig 4.9 Meshing of Impeller

The element type used for messing the impeller blade model is hexahedral. These hexahedral elements have six faces and eight corners. Four types of meshes, coarse, medium, fine and user defined, are available for the impeller.Fine meshes are more accurate than coarser meshes,but are very time consuming. Thats why I have choosen coarser mesh for this work.

Mesh Statistics

| | |
|---|---|
| Mesh type | Coarse |
| Number of Nodes | 295666 |
| Number of Elements | 276193 |
| Face Angle Range | 15 – 165 degree |
| Element Type | Hexahedra Brick Element |

.

### 4.8.3 Boundary Conditions

After developing the mesh model is exported to the CFX-Pre which is the preprocessing stage.At this stage the problem is formulated by providing initial conditions like boundary conditions,Domain physics,Running conditions etc

Initial conditions described below are provided as input to the pre-processor

Domain Physics for Impeller

| Location | Type | Material | Models |
|---|---|---|---|
| Passage | Fluid | Water | Turbulence Model = k epsilon<br>Turbulent Wall Functions = Scalable<br>Domain Motion = Rotating |

| | |
|---|---|
| Flow Direction | Normal to Boundary Condition |
| Relative Pressure | 1 [atm] |
| Turbulence | Medium Intensity |
| Wall Influence On Flow | No Slip |
| Wall Roughness | Smooth Wall |

After applying the boundary conditions,the problem is solved by solver.After getting the solutions they are post-processed using CFX-Post.

# CHAPTER 5
# STRESS ANALYSIS USING FEM

## 5.1 Introduction

FEM has become a powerful tool for numerical solution of wide range of engineering problems. Application range from deformation and stress analysis of automotive, aircraft, building , and bridge structures to field analysis of heat flux, fluid flow , magnetic flux, seepage, and other flow problems . With the advances in computer technology and CAD systems, complex problems can be modeled with relative ease. Several alternative configurations can be tried out on a computer before the first prototype is built. In this method of analysis, a complex region defining a continuum is discretized into simple geometric shapes called finite elements and expressed in terms of unknown values at element corners. An assembly process, duly considering the loading and constraints, results in set of equations. Solution of these equations gives us the approximate behavior of the continuum.

In the finite element method, the boundary and interior of the region are subdivided by lines (or surfaces) into a finite number of discrete sized subregions or finite elements. A number of nodal points are established with the mesh. These nodal points can lie anywhere along, or inside, the subdividing mesh, but they are usually located at intersecting mesh lines (or surfaces). The elements may have straight boundaries and thus, some geometric approximations will be introduced in the geometric idealization if the actual region of interest has curvilinear boundaries. The nodal points and elements are assigned identifying integer numbers beginning with unity and ranging to some maximum value. The assignment of the nodal numbers and element numbers will have a significant effect on the solution time and storage requirements. The analyst assigns a number of generalized degrees of freedom to each and every node. These are the unknown nodal parameters that have been chosen by the analyst to govern the formulation of the problem of interest. Common nodal parameters are displacement

components, temperatures, and velocity components. The nodal parameters do not have to have a physical meaning, although they usually do.

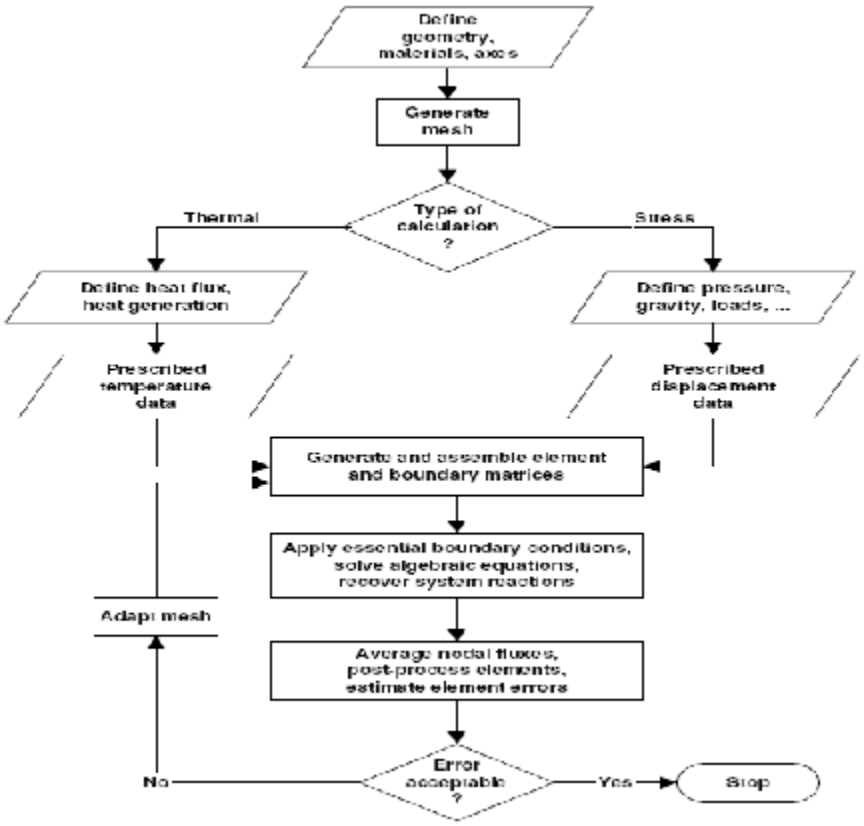


Fig 5.1 Flow diagram of FEM analysis

| Application | Primary | Associated | Secondary |
|---|---|---|---|
| Stress analysis | Displacement,<br>Rotation | Force,<br>Moment | Stress,<br>Failure criterion<br>Error estimates |
| Heat transfer | Temperature | Flux | Interior flux<br>Error estimates |
| Potential flow | Potential function | Normal velocity | Interior velocity<br>Error estimates |
| Navier-Stokes | Velocity | Pressure | Error estimates |
| Eigen-problem | Eigenvalues | Eigenvectors | Error estimates |

Fig 5.2 Primary and Secondary Variables in FEM

| Application | Given | Reaction |
|---|---|---|
| Stress analysis | Displacement | Force |
| | Rotation | Moment |
| | Force | Displacement |
| | Couple | Rotation |
| Heat transfer | Temperature | Heat flux |
| | Heat flux | Temperature |
| Potential flow | Potential | Normal velocity |
| | Normal velocity | Potential |
| Navier-Stokes | Velocity | Force |

Fig. 5.3 Reactions in FEM

## 5.2 Stresses

Stress solutions allow us to predict safety factors, stresses, strains, and displacements given the model and material of a part or an entire assembly and for a particular structural loading environment.A general three-dimensional stress state is calculated in terms of three normal and three shear stress components aligned to the part or assembly world coordinate system.The principal stresses and the maximum shear stress are called invariants; that is, their value does not depend on the orientation of the part or assembly with respect to its world coordinate system. The principal stresses and maximum shear stress are available as individual results.The principal strains $\varepsilon_1$, $\varepsilon_2$, and $\varepsilon_3$ and the maximum shear strain $\gamma_{max}$ are also available. The principal strains are always ordered such that $\varepsilon_1 > \varepsilon_2 > \varepsilon_3$. As with principal stresses and the maximum shear stress, the principal strains and maximum shear strain are invariants.

### 5.2.1 Von Mises stress

Von Mises stress is used as a criterion in determining the onset of failure in ductile materials. The failure criterion states that the von mises stress $\sigma_{vm}$ should be less than the yield stress $\sigma_y$ of the material. In the inequality form, the criterion may be put as

$$\sigma_{vm} \leq \sigma_y$$

The Von Mises stress is given by

$$\sigma_{vm} = ( I_1^2 - 3I_2 )^{1/2}$$

Where $I_1$and $I_2$ are the first two invariants of the stress tensor. For the general state of stress given by Eq. I1and I2 are given by

$$I_1 = \sigma_x + \sigma_y + \sigma_z$$

$$I_2 = \sigma_x\sigma_y + \sigma_y\sigma_z + \sigma_z\sigma_x - \tau^2_{yz} - \tau^2_{xz} - \tau^2_{xy}$$

In terms of the principal stresses σ1, σ2, and σ3, the two invariants can be written as

$$I_1 = \sigma_1 + \sigma_2 + \sigma_3$$

$$I_2 = \sigma_1\sigma_2 + \sigma_2 + \sigma_3\sigma_1$$

It is easy to check that Von Mises stress given in Previous equation can be expressed in the form

$$\sigma_{vm} = 1/\sqrt{2}\ ((\sigma_1 - \sigma_2)^2 + (\sigma_2 - \sigma_3)^2 + (\sigma_3 - \sigma_1)^2 )^{1/2}$$

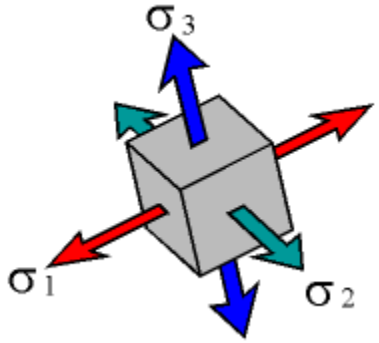


Fig 5.4 Principal Stresses

### 5.2.2 Total Deformation

A three dimensional body occupying a volume V and having a surface S is shown points in the body are located by x, y, z coordinates. The boundary is constrained on some region, where displacement is specified . On part of the boundary, distributed force per unit area T, is also called traction, is applied. Under the force, the body deforms. The deformation of a point x (=$[x,y,z]^T$ ) is given by the three components of its displacement:

$$u = [u,v,w]^T$$

The distributed force per unit volume , for example, the weight per unit volume , is the vector f given by

$$f= [f_x,f_y,f_z]^T$$

The body force acting on the elemental volume dV is shown in fig. The surface traction T may be given by its component values at points on the surface:

$$T= [T_x,T_y,T_z]^T$$

Examples of traction are distributed contact forces and action of pressure. A load P acting at a point i is represented by its three components:

$$P_i = [ P_x,P_y,P_z ]^T$$

The stresses acting on the elemental volume dV are shown in Fig. When the volume dV shrinks to a point, the stress tensor is represented by placing its components in a [3×3] matrix. However ,we represent the stress by the six independent components as in

$$\sigma = [ \sigma_x , \sigma_y , \sigma_z , \tau_{yz} , \tau_{xz} , \tau_{xy} ]^T$$

where $\sigma_x$ , $\sigma_y$ , $\sigma_z$ are normal stresses and $\tau_{yz}$ , $\tau_{xz}$ , $\tau_{xy}$ , are shear stresses. Let us consider equilibrium of the elemental volume shown in fig. First we get forces on faces by multiplying the stresses by the corresponding areas. Writing $\sum F_x = 0$, $\sum F_y = 0$,and $\sum F_z = 0$ and recognizing $dV= dxdydz$, we get equilibrium conditions

$$\frac{\partial \sigma_x}{\partial x} + \frac{\partial \sigma_y}{\partial y} + \frac{\partial \tau_{xz}}{\partial z} + f_x = 0$$

$$\frac{\partial \tau_{xy}}{\partial x} + \frac{\partial \sigma_y}{\partial y} + \frac{\partial \tau_{yz}}{\partial z} + f_y = 0$$

$$\frac{\partial \tau_{xz}}{\partial x} + \frac{\partial \tau_{yz}}{\partial y} + \frac{\partial \sigma_z}{\partial z} + f_z = 0$$

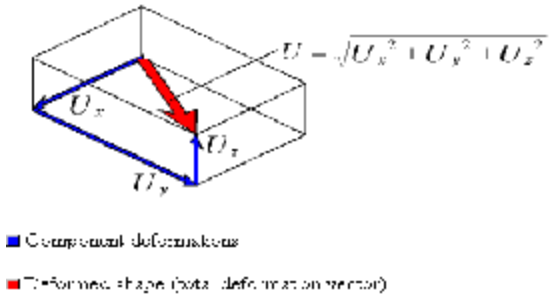


Fig 5.5 Total Deformation

## 5.3 Stress Analysis of Impeller using Ansys SIMULATION module

After getting the solutions from Ansys-CFX.The results are further used in Ansys-Simulation module for stress analysis of impeller.Pressure distributions which we obtain from CFX output are used as pressure input for the stress analysis of impeller due to impact of fluid on the surface of impeller.These analysis have been done on three different Rotational velocities i.e 1050 RPM,1250 RPM and 1450 RPM.Procedure to solve this problem is discussed below.

**Impeller Model**

Same Impeller model exported to simulation which we generated during CFX analysis.In simulation module there is an option by using that we can easily use any component of impeller like blade,hub etc. for analysis .In this work complete impeller and single blade fhave been analysed to check the effect of stress on single blade as well as whole impeller.

## Pre-Processing

**Material Assigned**

Material used was Iron

Properties of Iron

**a) Structural**

| | |
|---|---|
| Young's Modulus | 1.1e+005MPa |
| Poisson's Ratio | 0.28 |
| Density | 7.2e-006 kg/mm |
| Thermal Expansion | 1.1e-005 1/deg. C |
| Tensile Yield Strength | 0 MPa |
| Compressive Yield Strength | 0 MPa |
| Tensile Ultimate Strength | 240 MPa |
| Compressive Ultimate Strength | 820 MPa |

**b) Thermal**

| | |
|---|---|
| Specific Heat | 875J/kg deg. C |
| Thermal conductivity | 5.2e-002 W/mmdeg c |

**Meshing**

Same model which was meshed in turbogrid is used here.

**Rotation and Displacement**

In this analysis proper displacement and rotational constraints were provide.Displacement of model was constrained in X,Y and Z direction.Rotation was kept free about Z-axis and was kept fixed about X and Y axis.The arrow in fig is showing the direction of rotation

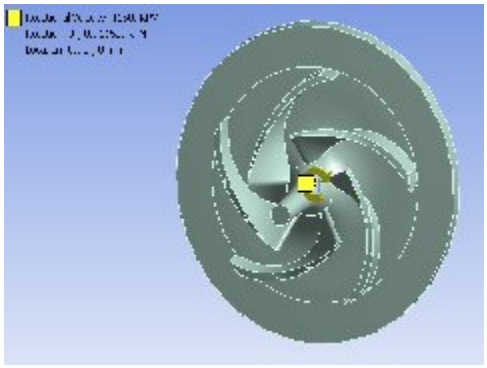

Fig 5.6 Rotational about Z-axis

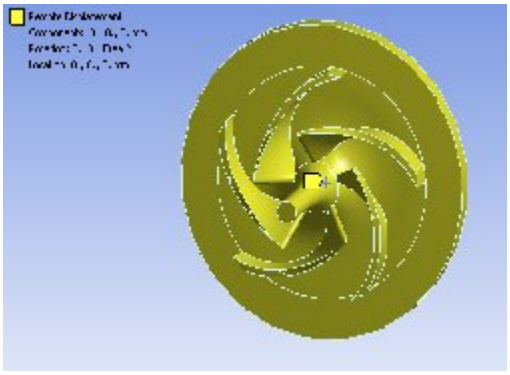

Fig 5.7 Fixed Displacement in X,Y,Z direction

During single blade analysis the side of blade which is attached with the hub was kept fixed which is shown in Fig 5.8.Rotation was kept free about Z- axis and was kept fixed about X and Y axis. The arrow in fig 5.7 is showing the direction of rotation and the blue side is showing the fixed side of blade.

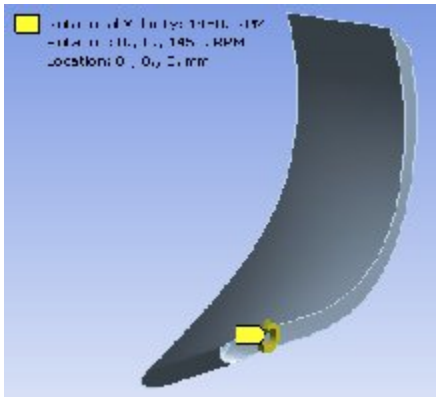

Fig 5.8 Rotational about Z-axis

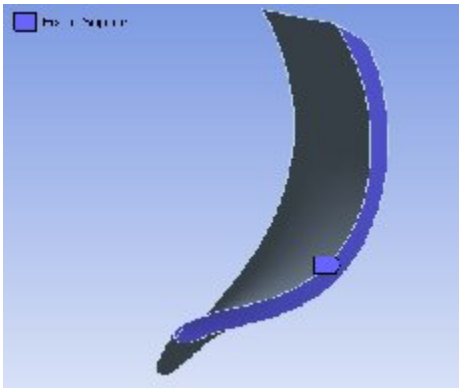

Fig 5.9 Fixed Displacement in X,Y,Z direction

**Loading**

After properly constraining the model CFX- loads and Centrifugal loads were applied.CFX loads are the loads which is calculated using Ansys-CFX.This is actually the pressure distribution of fluid over the surface of blade.CFX loads are shown in fig. .CFX loads are applied on the flat surface of blade as shown in fig. .The Red surface in Fig I showing the surface over which these loads are applied. Centrifugal forces were applied about Z-axis. Magnitude used was 1050 RPM, 1250 RPM, and 1450RPM.

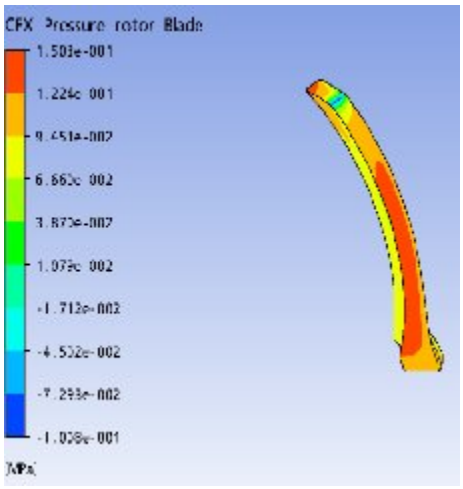


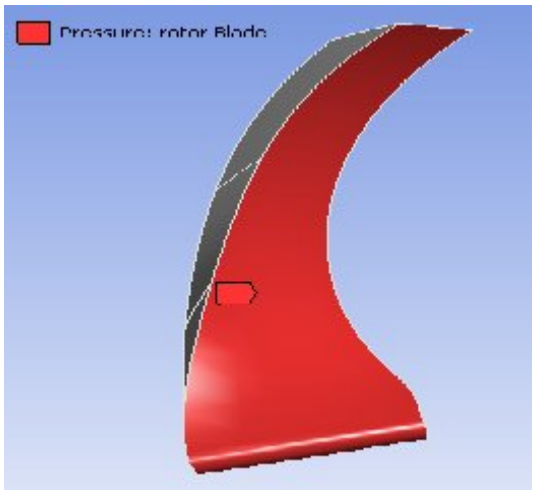

Fig.5.10 Pressure Distribution on Blade Fig 5.11 Surface on which Pressure is applied

## 5.3.3 Solution

After properly constraining and loading Von-Mises Stresses and Total Deformation were selected as a solution,and than solution was run.

## 5.3.4 Post-processing

Post processing shows the stress and deformation results at each node. Which is analysed to check whether the results are in safe limit or not.

# CHAPTER-6

# RESULTS AND DISCUSSIONS

.Results the distribution of pressure and stress of the impeller are discussed below.

## 6.1 Pressure distribution

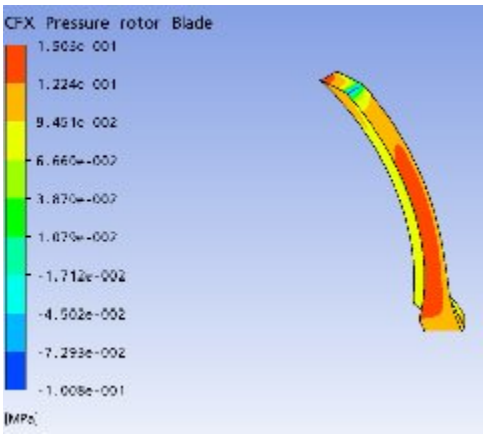


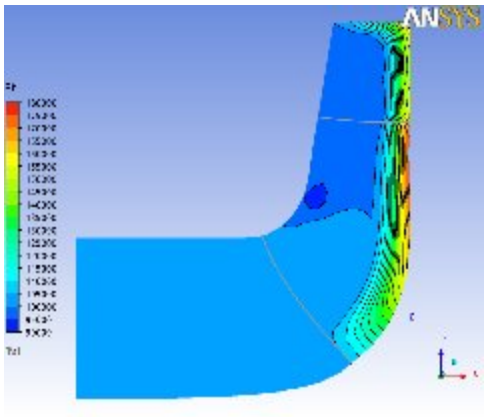


Fig 6.1 Pressure distribution at blade Fig 6.2 Pressure distribution at meridional surface

Fig.6.1 and 6.2 shows that pressure is minimum at the inlet in suction side and it keeps on increasing gradually and is maximum at the centre of the blade.

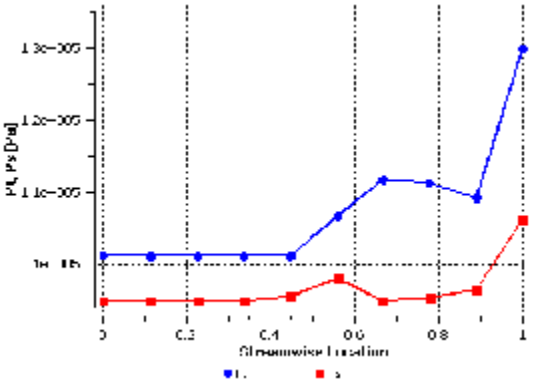

Fig 6.3 Pressure VS streamwise locations

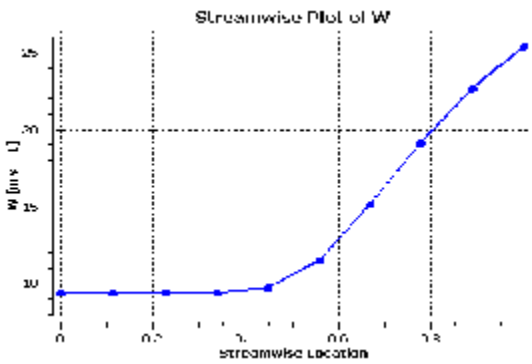


Fig 6.4 Velocity VS streamwise locations

Fig 6.3 & Fig 6.4 shows that the pressure and velocity distribution along streamwise location , and with increases the streamwise location pressure and velocity increases.

## 6.2 Stress and Deformation Analysis

### 6.2.1 Hub

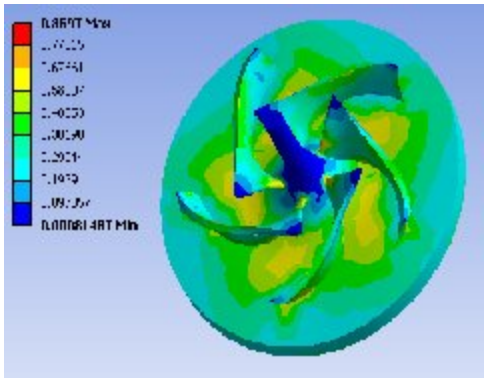

Fig 6.5 Stress distribution at 1050 RPM

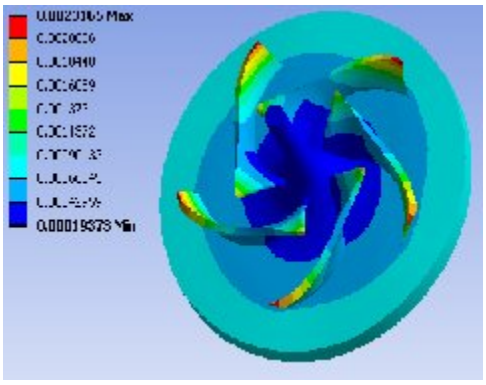

Fig 6.6 Total deformation at 1050 RPM

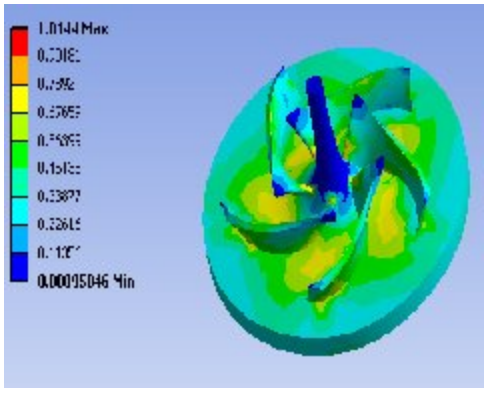

Fig 6.7 Stress Distribution at 1250 RPM

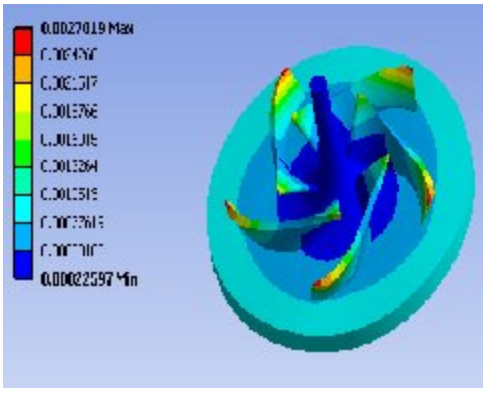

Fig 6.8 Total Deformation at 1250 RPM

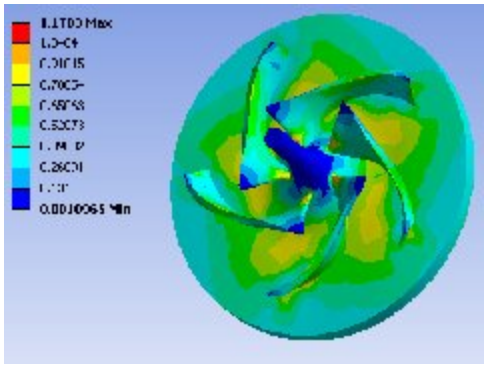

Fig 6.9 Stress Distribution at 1450 RPM

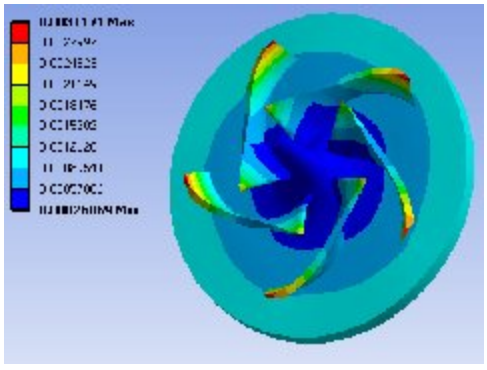

Fig 6.10 Total Deformation at 1450 RPM

Fig 5.5 & Fig 5.10 show that the stress and deformation distribution on the hub of the impeller at the 1050 rpm, 1250 rpm, 1450 rpm speed. The results show that stesses increases with speed, but are still under safe limit .

**Graphs for Hub Analysis**

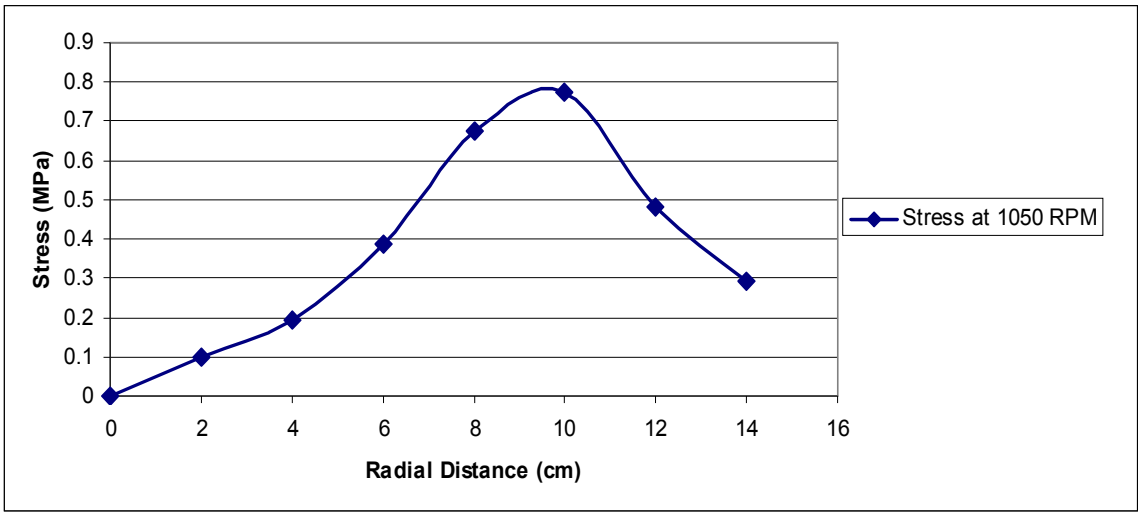


Fig 6.11 Stress Vs Radial distance at 1050 RPM

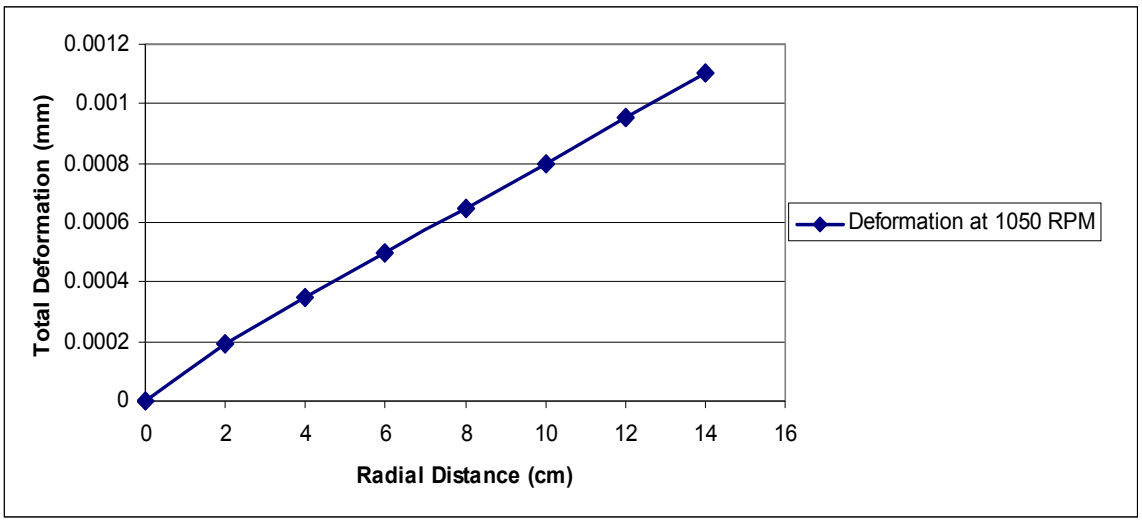


Fig 6.12 Deformation Vs Radial distance at 1050 RPM

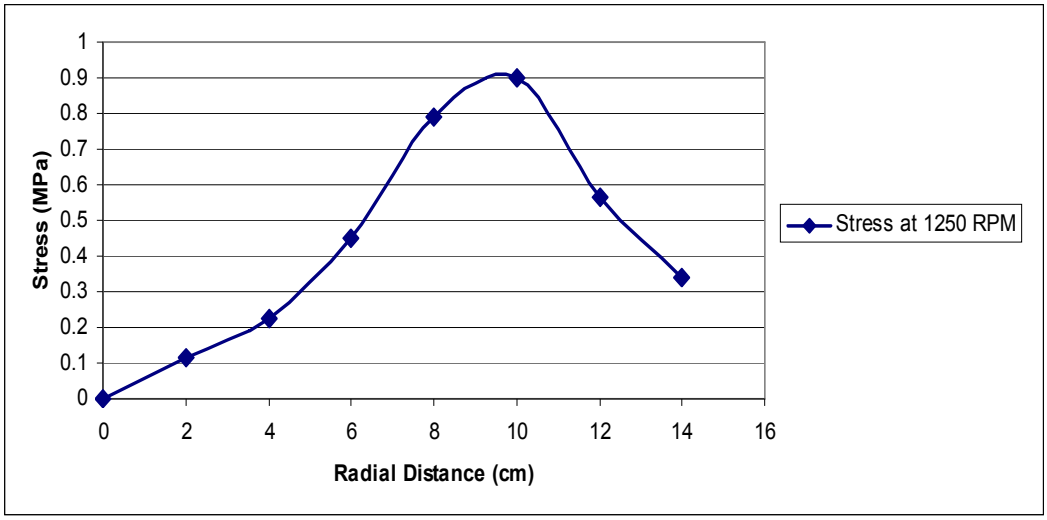


Fig 6.13 Stress Vs Radial distance at 1250 RPM

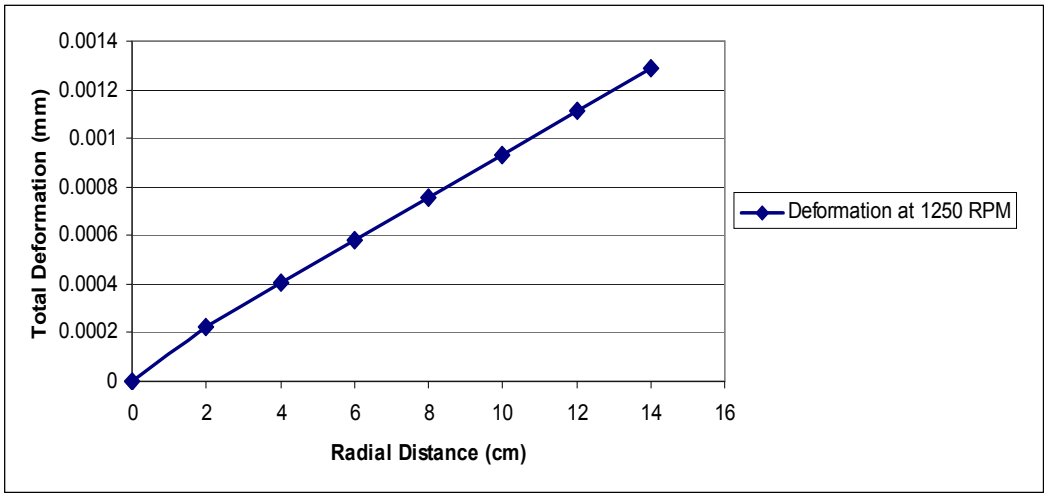


Fig 6.14 Deformation Vs Radial distance at 1250 RPM

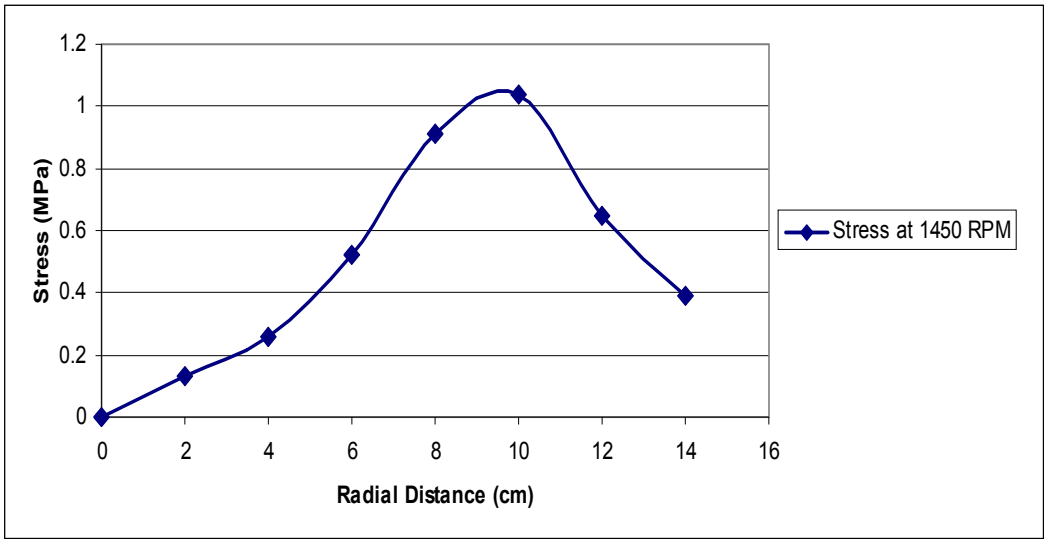


Fig 6.15 Stress Vs Radial distance at 1450 RPM

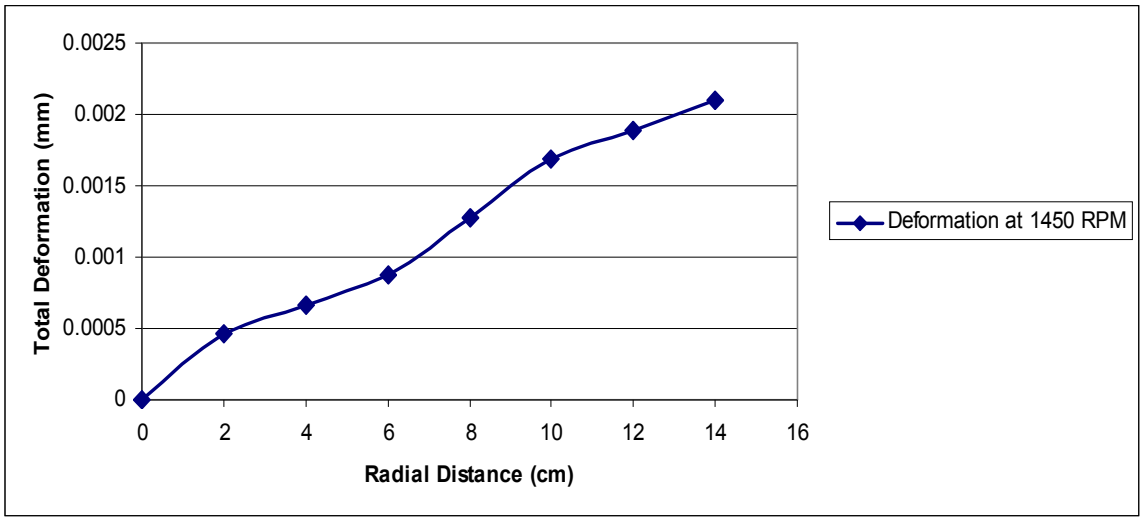


Fig 6.16 Deformation Vs Radial distance at 1450 RPM

### 6.2.2 Blade

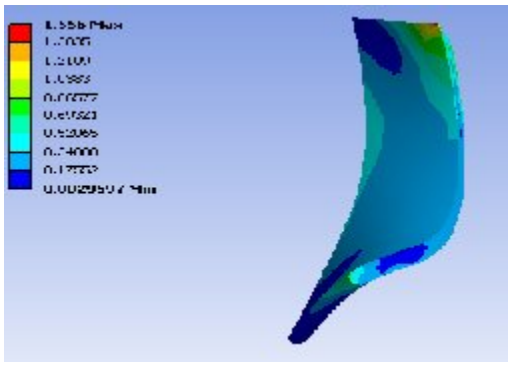

Fig 6.17 Stress distribution at 1050 RPM

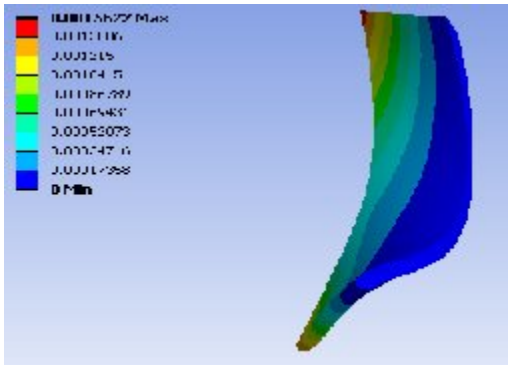

Fig 6.18 Total Deformation at 1050 RPM

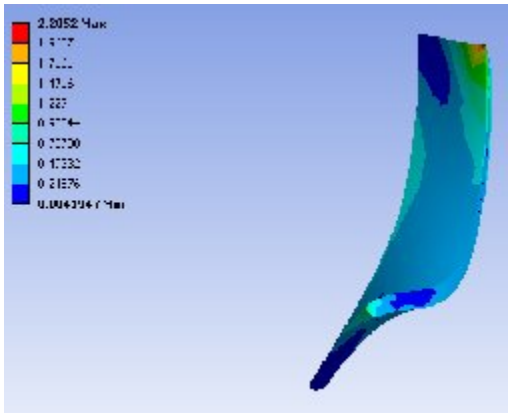

Fig 6.19 Stress Distribution at 1250 RPM

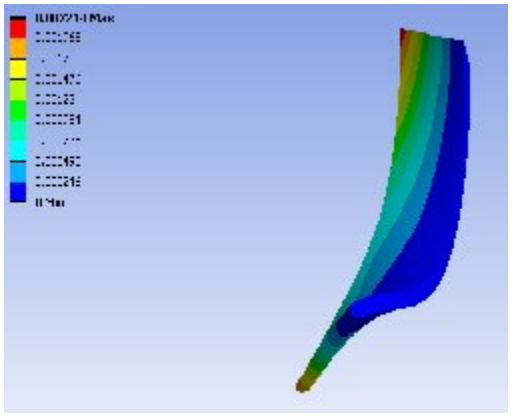

Fig 6.20 Total Deformation at 1250 RPM

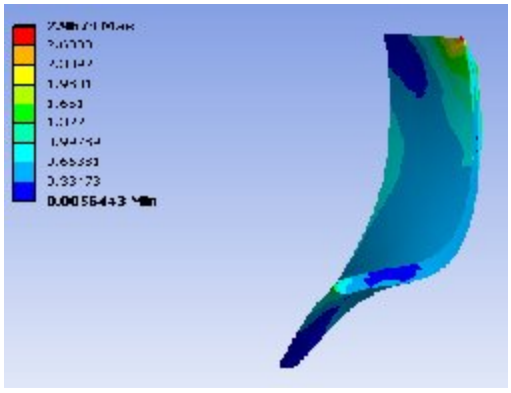

Fig 6.21 Stress Distribution at 1450 RPM

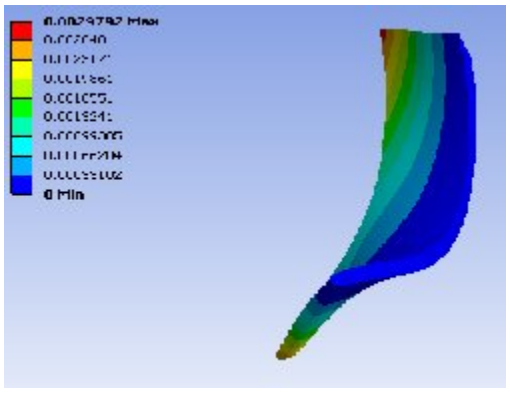

Fig 6.22 Total Deformation at 1450 RPM

Fig 5.17 & Fig 5.22 show that the stress and deformation distribution on the hub of the impeller at the 1050 rpm, 1250 rpm, 1450 rpm speed. The results show that stesses increases with speed, but are still under safe limit .

**Graphs for Blade Analysis**

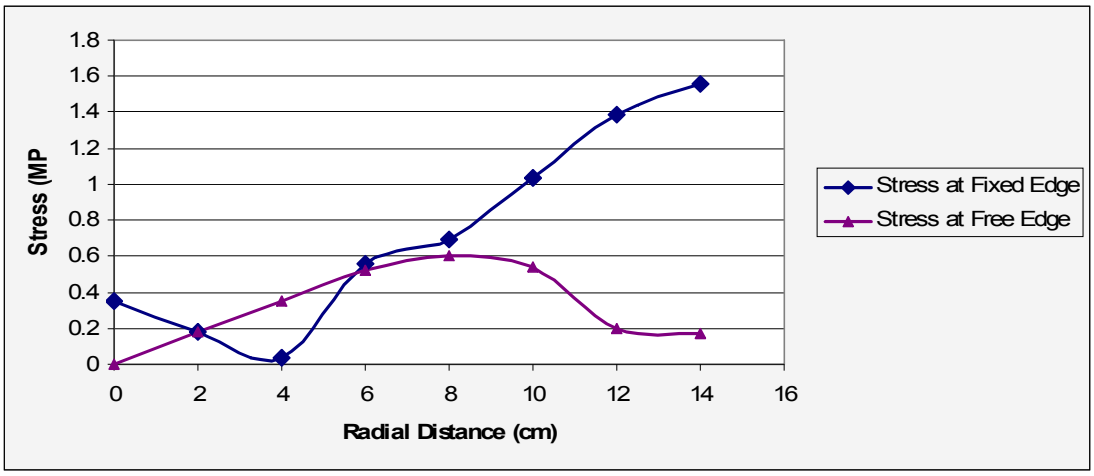


Fig 6.23 Stress VS Radial distance at 1050 RPM

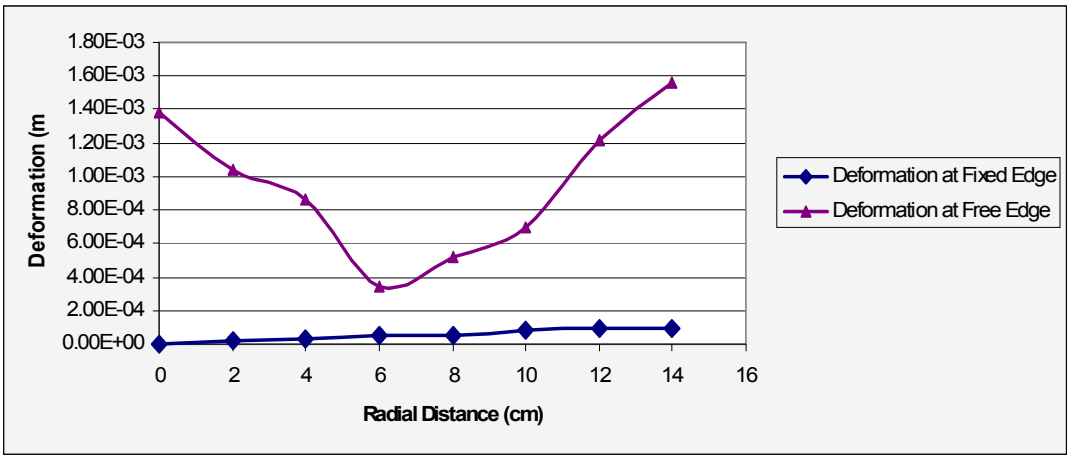


Fig 6.24 Deformation VS Radial distance at 1050 RPM

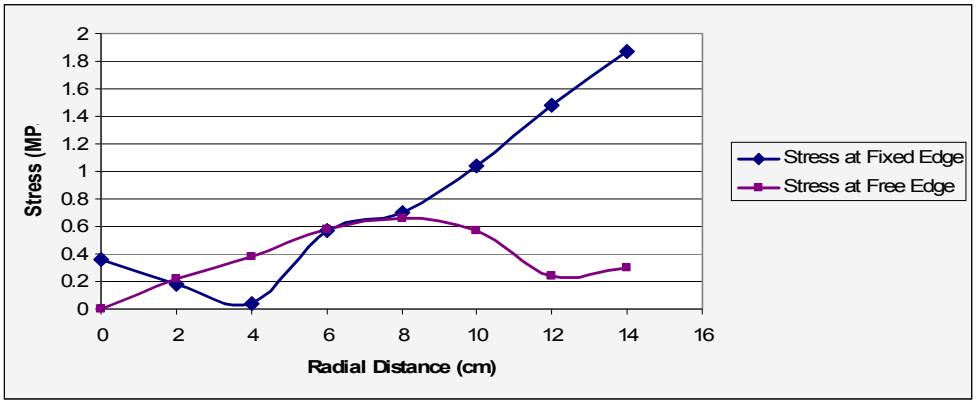


Fig 6.25 Stress VS Radial distance at 1250 RPM

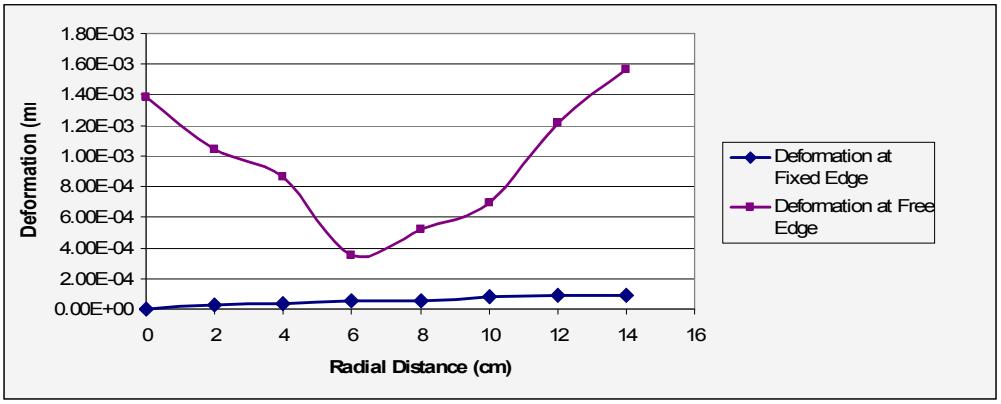


Fig 6.26 Deformation VS Radial distance at 1250 RPM

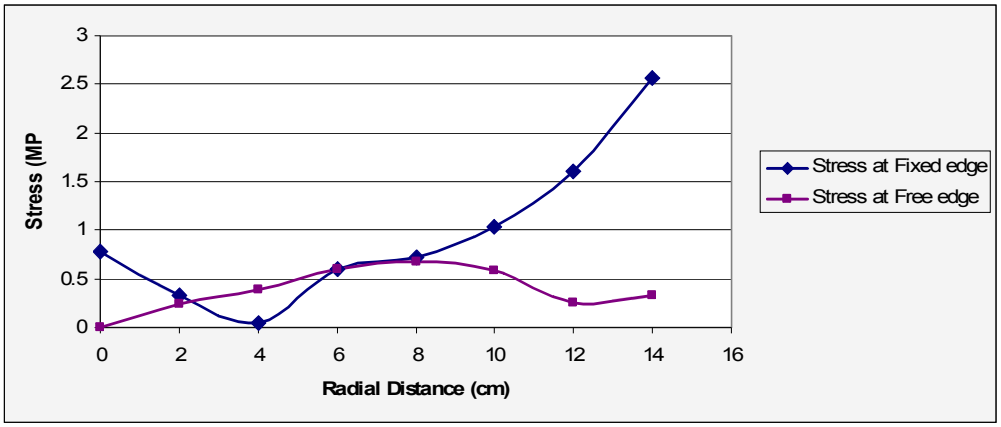


Fig 6.27 Stress VS Radial distance at 1450 RPM

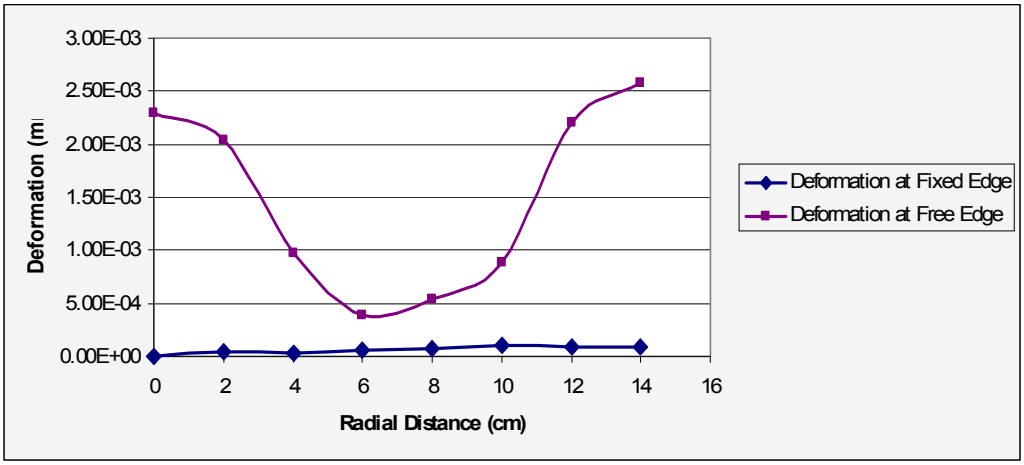


Fig 6.28 Deformation VS Radial distance at 1450 RPM

Figure 6.23-6.28 is showing that the side of blade which is fixed with hub is having more stress than the side which is free.similarly,deformation at side which is fixed is more than the side which is free.

# CHAPTER 7
# CONCLUSION AND SCOPE FOR FUTURE WORK

## 7.1 Conclusion

A numerical model of an impeller has been successfully generated and the complex internal flow fields are investigated by using the Ansys-CFX code. Simulation results are obtained at blade streamwise location, meridional surface.The pressure increases gradually along the stream wise direction. The regions in the impeller experiencing the maximum pressure were located at the outlet. At low flow rates strong recirculation of flow takes place in suction side of the blade, whereas the flow in pressure side is smooth. But as the flow rate increases the flow separation along the pressure side of the impeller blade takes place, which results in the recirculation of flow in the pressure side. Pump performance curves generated shows good agreement with the open literature. It is concluded that with the increase .Design program of the impeller has been developed for configuration of centrifugal pump for the consideration of pump efficiency. Advantage of computer permit the wide range of design variable to investigated in a very short time.Stress analysis of impeller was shown for given material is in safe limited conditions

## 7.2 Scope for future work

- Pressure and velocity distribution in the casing of pump can be analysed
- Same CFD method can be applied for calculating velocity and pressure in other turbo machinery components.

Further work can be taken up to see the effect of variation in clearance gaps like side spacing between impeller and casing, volute tongue clearance etc. on performance and wear characteristics of pumps.

# REFERENCES


1. V. P. Vasandhani, D. S. Hira, (1975) "Influence Of Volute Tongue Length and Angle on the Pump Performance" IE Journal-ME Volume 56, July 1975.

2. Jaroslaw Mikielewicz, David Gardon Wilson, Tak-Chee Chan and Albert L. Goldfinch, (1978), " A Method for Correlating the Characteristics of Centrifugal Pumps in Two-Phase Flow" Journal of fluids Engineering, December 1978, Vol 10.

3. J.W Crisswell, (1982), ''Practical Problems Associated With Selection and Operation of Slurry Pumps'' Proc.Hydrotransport-8, Paper H1, BHRA Fluid Engineering, pp 317-338

4. J. Remisz, Dr. eng., (1983) "Slurry Pumps: Transformation Of Characteristics And Design" Eiththh Conference of British Pump Manufacturers Association©BHRA Fluid Engineering 1983.

5. Mez, W., (1984), ''The Influence of Solid Concentration, Solid Density and Grain Size Distribution on the Working Behavior of Centrifugal Pumps,'' Proc.Hydrotransport-9, Paper H1, BHRA Fluid Engineering, pp. 345–358.

6. Walker, C. I., and Goulas, A., (1984), ''Performance Characteristics of Centrifugal Pumps When Handling Non-Newtonian Homogeneous Slurries,'' Proc. Instn.Mech. Engrs., **198A**, pp. 41–49.

7. Koji Kikuyama ,Murakami M,Asakuru E,Osuka T,Jinsheng,(1985), ''Velocity Distribution In The Impeller Passages of Centrifugal Pumps'',Bulletin of JSME,Vol 28,No. 243,September 1985.

8. Sheth, K. K., Morrison, G. L., and Peng, W. W., (1987), ‘‘Slip Factors of Centrifugal Slurry Pumps,’’ ASME J. Fluids Eng., **109**, pp. 313–318.

9. M A Rayan, M Shawky,(1989),‘‘Evaluation Of Wear In a Centrifugal Slurry Pump’’1989 Proc Instn Mech Engrs Vol 203

10. Dong, R., Chu, S., and Katz, J., (1992), ‘‘Quantitative Visualization of the Flow within the Volute of a Centrifugal Pump. Part A: Technique,’’ASME J. Fluids Eng., **114** pp. 390–395

11. Gahlot, V. K., Seshadri, V., and Malhotra, R. C. (1992), ‘‘Effect of Density, Size Distribution, and Concentration of Solid on the Characteristics of Centrifugal Pumps.’’ J. Fluids Eng., ASME Vol 114, 386–389.

12. Cader, T., Masbernat, O., and Roco, M.C., (1992), ‘‘LDV Measurements in a Centrifugal Slurry Pump: Water and Dilute Slurry Flow,’’ ASME J. Fluids Eng., **114**, pp. 606–615.
13. Cader, T., Masbernet, O., and Roco, M. C., (1994), ‘‘Two-Phase Velocity Distributions And Overall Performance of a Centrifugal Slurry Pump,’’ ASME J.Fluids Engineering Conf., Washington, DC, June 20–24. **116**, pp. 176–186.

14. W.Huang,T Cader ,M C Roco,(1995), ‘‘Two Phase Flow Structure at The Impeller-Volute Interface ’’April 3-7,1995,Proceedings Of The 2nd International Conference On Multiphase Flow,Kyoto Japan.

15. S .Yedidiah (1996). ‘‘Present Knowledge of the Effects Of The Impeller Geometry On The Developed Head ’’ 1996, Proc Instn Mech Engrs Vol 210.

16. S.Yedidiah, (1996),”A New Toll for Solving Problems Encountered with Centrifugal Pumps”April 1996 world Pumps Elsevier science.

17. Ni, F, Vlasblom, W. J., and Zwartbol, A. (1999), ‘‘Effect of High Solid Concentration on Characteristics of a Slurry Pump,’’ Hydrotransport 14, BHRA Fluid Engg. Maastricht, The Neatherland, pp. 141–149.
18. Miner, S. M., (1997), “3-D Viscous Flow Analysis of an Axial Flow Pump Impeller” International Journal of Rotating Machinery, Volume 3, No. 3, pp 153-161.

19. S. Gopalkrishnan, (1999) “ Pump Research and Development: Past, Present, and Future- An American Perspective” 1999 Journal of fluid engineering, ASME.

20. Oh and M.K. Chung (1999), “Optimum values of design variables versus specific speed for centrifugal pumps”. Proc Instn Mech Engrs Vol. 213 ,1999

21. Anders Sellgren,Graeme Addie and Stephen Scott,(2000),”The Effect of Sand-Clay Slurries on the Performance of centrifugal pump”,The Canadian journal of Chemical Engineering,Vol – 78.

22. B.K Gandhi, S.N. Singh, V. Seshadri, (2001) “ Variation of Wear along the Volute Casing of a Centrifugal Slurry Pump”. JSME International Journal Vol. 44, 2001.

23. Gandhi, B. K., Singh, S. N., and Seshadri, V., (2001), ‘‘Performance Characteristics of Centrifugal Slurry Pumps,’’ ASME J. Fluids Eng., **123**, pp. 271–28.

24. Cader, T., Masbernat, O., and Roco, M.C., (2001), ‘‘LDV Measurements in a Centrifugal Slurry Pump: Water and Dilute Slurry Flow,’’ ASME J. Fluids Eng., **114**, pp. 606–615.

25. Oh and Kim, (2001) “Conceptual Design, Optimiztion of mixed-flow pump impellers using mean streamline analysis”. Proc Instn Mech Engrs Vol. 215,2001

26. K S Paeng, M K Chung,(2001),"A New Slip Factor For Centrifugal Impellers",Proc Instn Mech Engrs Vol 215 Part A.

27. Engin, T., and Gur, M., (2001), ''Performance Characteristics of a Centrifugal Pump Impeller with Running Tip Clearance Pumping Liquid-Solid Mixtures,''ASME J. Fluids Eng., **123**, pp. 532–538.

28. Bross, S., Addie, G.R., (2002), "Prediction of Impeller Nose Wear Behaviour in Centrifugal Slurry Pumps," 4th International Conference on Mulitphase Flow, New Orleans, LA, USA

29. B.K Gandhi, S.N. Singh, V. Seshadri, (2002) "Effect of Speed on the Performance Characteristics of a Centrifugal Slurry Pump", Journal of fluid Engineering, Vol. February 2002.

30. Akira Goto, Motohiko Nohmi, Takaki Sakurai, Yoshiyasu Sogawa, (2002) " Hydrodynamic Design System for Pumps Based on 3-D CAD, CFD, and inverse Design Method" published by EBARA Corporation, Tokyo, Japan.

31. Tahsin Engin, Mesut Ger., (2003)," Comparative Evaluation of Some Existing Correlations to Predict Head Degradation of Centrifugal Slurry Pumps", Journal of fluid Engineering, Vol. January 2003.

32. J R.Kadambi,Charoenngam P,Subramanian A, Mark P.Wernet,John M.Sankovic, Addie G, Courtwright R(2004),"Investigation of Particle Velocities in a Slurry pump using PIV:Part 1,The Tongue and Adjacent Channel Flow" Journal Of Energy Resources Technology,ASME. December 2004 Vol-126/271.

33. Graeme R. Addie, J. R. Kadambi, Robert Visintainer , (2005) " Design and application, slurry pump technology" 2005 ASME Fluids engineering summer conference Houston, Texas, June 19-23 2005. G.R Addie,A.S Roundnev and
34. A.Sellgren,(2007),"The new ANSI/HI centrifugal slurry pump standard", 17th International conference on the hydraulic transport of solids,The southern African Institute of Mining and Metallurgy and the BHR group

35. L.Pullum,L.J.W Graham and M.Rudman,(2007),"Centrifugal pump performance calculations for homogeneous and complex heterogeneous suspensions",17th International conference on the hydraulic transport of solids,The southern African Institute of Mining and Metallurgy and the BHR group.

36.Min-Guan Yang,Dong Liu,Xiang Dong,(2007)"Analysis of turbulent Flow in the Impeller of a Chemical Pump",Journal of engineering science and technology,Vol-2,N0.- 3,2007,Pg-218-225

# Bibliography

37.Stepanoff, A. J., (1958), "Centrifugal and axial flow pumps theory design and application", 2nd ed, John wilay and sons, New York.
38. Vasandani, V. P., (1993), "Hydraulic machines theory and design", 10th edition, Khanna Publishing house, New Delhi.
39 .Jagdish Lal, (1998), "Hydraulic Machines", Metropolitan Book Co. India
40. Satish Kumar,(2006) "A textbook of Fluid Mechanics". Dhanpat Rai Publications.
41 .Kalyanmoy Deb,(1996), "Optimization for Engg. Design".
42. Richard L. Fax, (1994),"Optimization methods for Engg. Design" .
43. Kanetkar, Y. P., (2002), "Let us C", BPB publications, New Delhi.
44. Balagurusamy, E., (2005), "Programming in C#", Tata McGraw-Hill, New Delhi.
45 ANSYS CFX-Manual, (2006), Published by, ANSYS CFX, Release 11.0, December, 2006, ANSYS, Inc.
46 Ghoshdastidar, P. S., (1998), "Computer simulation of flow and heat transfer", Tata McGraw-Hill, New Delhi.

# ANNEXURE I

# PROGRAM FOR DESIGN OF CENTRIFUGAL PUMP

```
                        /* Design of impeller*/

#include<stdio.h>
#include<conio.h>
#include<math.h>
double  sai= 0.58 ;
double  fi = 0.175;
double  eta= 0.78;
double  g  = 9.8;
double  ro = 1000;
double  pi = 3.14;
double sigma =0.66;
void main()
    {  double H,z,b2,N,Q,P,Ns,D2,U2,Psh,Dhb,Dsh,De,Vm1,D1,U1,B1,B2,Z,B,Ku;
          double V1,Vr1,Vm2,W1,Vrui,Vr2,Alpha2,V2,Vu2;
          double Re,Fd,Vth,Vd,S,Ath,HL,sigb,NPSHR;
          char ch;
          clrscr();

          printf("\n New session of calculating :: \n Following variables ::\n1-Ns\n2-U2\n3-
D2\n");
          printf("Values of the constants taken are :::\n ");
          printf("sai =%lf\nfi=%lf\n eta=%lf\ng=%lf\nro=%lf\n",sai,fi,eta,g,ro);
          printf("\nThe value  of Sigma=%lf",sigma);


          printf("\nPress any key to go ahead");
          getch();
          printf("For Calculation pls Enter following value");

          printf("\nH====");
          scanf("%lf",&H);

          printf("\nN====");
          scanf("%lf",&N);

          printf("\nQ====");
          scanf("%lf",&Q);
```

```
        Ns= (N * sqrt(Q))/pow(H,0.75);


        U2=sqrt((g*H)/(eta*sai));

        D2 = (60 * U2)/ ( pi * N);
        printf("\npress any key to get results");
        getch();

        printf("\nValues obtained are =>>\n1-Ns=%lf\n2-U2=%lf\n3-
D2=%lf\n",Ns,U2,D2);


    //  printf("\nDo you want more processing Y/N\n");

    //  scanf("%c",&ch);

    //  if(ch!='Y' && ch!='y')
    //  return;

        P=(ro*g*Q*H)/(eta*735);

        Psh=1.14*P;

        Dsh =0.12*pow((Psh/N),0.33);


        Dhb= Dsh*1.2;
     //  if(0.020<Dsh<=0.100)
     //  Dhb= Dsh +.016;
        Vm1 = fi*U2;

        De = (Q*4)/(Vm1*pi) + pow(Dhb,2);
        De = sqrt(De);

        D1 = De + 0.020;
        Vm2 = 1.15*Vm1;
        U1 = (pi*D1*N)/60;
        W1=Q/(pi*D2*Vm2);
        B1 = atan(Vm1/U1);
        B1 = (B1 *180)/pi;
        printf("\nValues calculated are =\n P=%lf\n Psh=%lf\n Dsh=%lf\nDhb=%lf\n
Vm1=%lf\n De=%lf\n D1=%lf\n U1=%lf\n
B1=%lf\n",P,Psh,Dsh,Dhb,Vm1,De,D1,U1,B1);
     //   printf("Do you want more processing Y/N\n");
    //  scanf("%c",&ch);
```

```
  //      if(ch!='Y' && ch!='y')
    //    return;


          b2 = atan((sigma - sai)/fi);

          b2= (b2*180)/pi;
          z= b2/3;
          printf("\nValues calculated are =\n B2=%lf\n z=%lf\n",b2,z);
   /*************************************************************/

   V1=Vm1;
    Vr1=(U1*U1 + Vm1*Vm1);
    Vr1=sqrt(Vr1);
    Vrui=U1;
    Vr2=Vm2/(sin(b2));
    Alpha2=atan(Vm2/(U2-Vr2*(cos(b2))));
    V2=(Vm2/(cos(Alpha2)));
    Vu2=(U2-Vr2*cos(b2));
    printf("Values calculated
are\nW1=%lf\nVm2=%lf\nV1=%lf\nVr1=%lf\nVrui=%lf\nVr2=%lf\nAlpha2=%lf\nV2=
%lf\nVu2=%lf\n",W1,Vm2,V1,Vr1,Vrui,Vr2,Alpha2,V2,Vu2);

   /*************************************************************/
     getch();
     return;
  }
```

/* Design of valute casing*/

```
#include<stdio.h>
#include<conio.h>
#include<math.h>
double ALPHA3 =8.13;
double  sai= 0.58 ;
double  fi = 0.175;
double  eta= 0.78;
double  g  = 9.8;
double  ro = 1000;
double  pi = 3.14;
double sigma =0.66;
```

```
void main()
    {  double H,z,b2,N,Q,P,Ns,D2,U2,Psh,Dhb,Dsh,De,Vm1,D1,U1,B1,B2,Z,B,Ku;
          double V1,Vr1,Vm2,W1,Vrui,Vr2,Alpha2,V2,Vu2;
          double Re,Fd,Vth,Vd,S,Ath,HL,sigb,NPSHR,D3,B3,Rv,Bx,thita,Vthx,Vu3;
          char ch;
          clrscr();

          printf("\n New session of calculating :: \n Following variables ::\n1-Ns\n2-U2\n3-
D2\n");
          printf("Values of the constants taken are :::\n ");
          printf("sai =%lf\nfi=%lf\n eta=%lf\ng=%lf\nro=%lf\n",sai,fi,eta,g,ro);
          printf("\nThe value  of Sigma=%lf",sigma);


          printf("\nPress any key to go ahead");
          getch();
          printf("For Calculation pls Enter following value");

          printf("\nH====");
          scanf("%lf",&H);

          printf("\nN====");
          scanf("%lf",&N);

          printf("\nQ====");
          scanf("%lf",&Q);


          Ns= (N * sqrt(Q))/pow(H,0.75);


          U2=sqrt((g*H)/(eta*sai));

          D2 = (60 * U2)/ ( pi * N);
          printf("\npress any key to get results");
          getch();

          printf("\nValues obtained are =>>\n1-Ns=%lf\n2-U2=%lf\n3-
D2=%lf\n",Ns,U2,D2);


    //    printf("\nDo you want more processing Y/N\n");

    //    scanf("%c",&ch);

    //    if(ch!='Y' && ch!='y')
```

```
    //     return;

           P=(ro*g*Q*H)/(eta*735);

           Psh=1.14*P;

           Dsh =0.12*pow((Psh/N),0.33);


           Dhb= Dsh*1.2;
      //   if(0.020<Dsh<=0.100)
      //   Dhb= Dsh +.016;
           Vm1 = fi*U2;

           De = (Q*4)/(Vm1*pi) + pow(Dhb,2);
           De = sqrt(De);

           D1 = De + 0.020;
           Vm2 = 1.15*Vm1;
           U1 = (pi*D1*N)/60;
           W1=Q/(pi*D2*Vm2);
           B1 = atan(Vm1/U1);
           B1 = (B1 *180)/pi;
           printf("\nValues calculated are =\n P=%lf\n Psh=%lf\n Dsh=%lf\nDhb=%lf\n
Vm1=%lf\n De=%lf\n D1=%lf\n U1=%lf\n
B1=%lf\n",P,Psh,Dsh,Dhb,Vm1,De,D1,U1,B1);

       //    printf("Do you want more processing Y/N\n");
      //     scanf("%c",&ch);

     //       if(ch!='Y' && ch!='y')
      //     return;


            b2 = atan((sigma - sai)/fi);

            b2= (b2*180)/pi;
            z= b2/3;
            printf("\nValues calculated are =\n B2=%lf\n z=%lf\n",b2,z);
    /*****************************************************************/

     V1=Vm1;
      Vr1=(U1*U1 + Vm1*Vm1);
      Vr1=sqrt(Vr1);
      Vrui=U1;
      Vr2=Vm2/(sin(b2));
```

```
    Alpha2=atan(Vm2/(U2-Vr2*(cos(b2))));
    V2=(Vm2/(cos(Alpha2)));
    Vu2=(U2-Vr2*cos(b2));
    printf("Values calculated
are\nW1=%lf\nVm2=%lf\nV1=%lf\nVr1=%lf\nVrui=%lf\nVr2=%lf\nAlpha2=%lf\nV2=
%lf\nVu2=%lf\n",W1,Vm2,V1,Vr1,Vrui,Vr2,Alpha2,V2,Vu2);


   /*************************************************************/
     getch();

          B3= 1.8 * W1;
          D3=1.15 * D2;
          Rv=(D2+D3)/4;
          Bx=B3+(2*(Rv-0.5*D2)/1.73);
          Vu3=V2*cos(ALPHA3);
          thita =log(D3/D2)/tan(Alpha2);
          Vthx=(D2*Vu2/D3);
          getch();
          printf("Values calculated are
\nB3=%lf\nD3=%lf\nRv=%lf\nBx=%lf\nVu3=%lf\nthita=%lf\nVthx=%lf\n",B3,D3,Rv,
Bx,Vu3,thita,Vthx);
          getch();
     return;
   }
```

**ANNEXURE II:**
**OUTPUT OF THE PROGRAM**

**Output of impeller dimensions**

| | | |
|---|---|---|
| 1 | Specific speed of pump | 25.78 rpm |
| 2 | Input power of the pump | 57.65 HP |
| 3 | Shaft Power | 65.72 HP |
| 4 | Diameter of shaft | 0.04 m |
| 5 | Hub Diameter | 0.05 m |
| 6 | Axial velocity | 2.5487 m/sec |
| 7 | Eye diameter | 0.14 m |
| 8 | Inlet blade diameter | 0.166305 m |
| 9 | Hub diameter | 0.02362 m |
| 10 | Width at inlet | 0.011342 m |
| 11 | Inlet blade velocity | 12.87 m/sec |
| 12 | Inlet blade angle | $21.8218^{\circ}$ |
| 13 | Outlet blade velocity | 29.43 m/sec |
| 14 | Outlet blade diameter | 0.388 m |
| 15 | Number of blades | 8 |
| 16 | Width of blade at outlet | 0.007678 m |
| 17 | NPSH required | 1.64 |
| 28 | Outlet blade angle | $24.58^{\circ}$ |